3–manifolds algorithmically bound 4–manifolds

by

Samuel Churchill
B.Sc., University of Victoria, 2013

A Thesis Submitted in Partial Fulfillment of the
Requirements for the Degree of

Master of Science

in the Department of Mathematics and Statistics

© Samuel Churchill, 2019
University of Victoria

3–manifolds algorithmically bound 4–manifolds

by

Samuel Churchill
B.Sc., University of Victoria, 2013

Supervisory Committee

_____

Dr. Ryan Budney, Primary Supervisor
(Department of Mathematics and Statistics)

_____

Dr. Alan Mehlenbacher, Co-Supervisor
(Department of Economics)

ABSTRACT

This thesis presents an algorithm for producing 4–manifold triangulations with boundary an arbitrary orientable, closed, triangulated 3–manifold. The research is an extension of Costantino and Thurston's work on determining upper bounds on the number of 4–dimensional simplices necessary to construct such a triangulation. Our first step in this bordism construction is the geometric partitioning of an initial 3–manifold M using smooth singularity theory. This partition provides handle attachment sites on the 4–manifold $M \times [0,1]$ and the ensuing handle attachments eliminate one of the boundary components of $M \times [0,1]$, yielding a 4-manifold with boundary exactly M. We first present the construction in the smooth case before extending the smooth singularity theory to triangulated 3–manifolds.

Contents

List of Figures

List of Algorithms

Chapter 1

Introduction

When we begin studying manifolds, we find the basic problems of surface theory rife with algorithms and elegant solutions. Moving up by one dimension, a core of algorithms cover 3–manifold theory. These algorithms, though sophisticated, are historically unexpected in form and possibly hard to implement, leading some to prefer more conceptually pleasant pseudo-algorithms such as SnapPy [5]. Many problems in high dimensions (5 and up) become impossible due to the complexities of the word problem in fundamental groups and the difficulties in resolving smoothing of CW-complexes. By comparison, the landscape of 4–manifold theory is not so easily generalized. High dimensional complications such as the word problem crop up, but dimension 4 is unique when considering the corresponding relation between CW complexes and smoothing theory. Moreover, algorithmic recognition of the n–sphere is resolved in every dimension but 4, where it is an open problem. Costantino & Thurston's results in shadow theory evoke traditional 3–manifold theory techniques, suggesting that some basic cobordism questions may not be computationally difficult in dimension 4.

Our assemblage of a constructive proof that 3–manifolds bound 4–manifolds was inspired by the discussion in Section 2.2 of Costantino & Thurston's "3–manifolds efficiently bound 4–manifolds" [4]. An appropriately well-behaved smooth map from a 3–manifold M to $\mathbb{R}^2$ induces a stratification of M into a union of handlebodies. This stratification serves as a set of surgery instructions for turning M into S^3. It can also be interpreted as a set of 4–dimensional handle attachment sites, and attaching these handles to one boundary component of $M \times [0, 1]$ produces a 4–manifold whose boundary is precisely M.

Our algorithm is the adaptation of this smooth proof to the setting of triangulated

manifolds. We define a map from the input 3–manifold triangulation to $\mathbb{R}^2$, subdivide the manifold into handlebodies, then attach handles to one boundary component of the manifold's 4–thickening until we obtain the desired outcome.

1.1   Expected Background

This document is aimed at a reader with some understanding of the tools of low–dimensional manifold theory. We do not present the basics of manifold theory, calculus on manifolds, or triangulations of manifolds.

For the fundamentals of manifolds and calculus on manifolds see Lee's "Introduction to Smooth Manifolds" [7]. For more on 3–manifolds and an introduction to triangulations, see Thurston's "Three-dimensional geometry and topology" [13].

1.2   Agenda

What follows is a brief summary of the contents of each chapter in this document. Each chapter has a purpose, and that purpose is also stated.

Chapter 1 lays out what the central thesis problem is and why it is interesting. It also sets expectations for the rest of the document in terms of what to expect and what not to expect.

Chapter 2 presents some specialized tools of low–dimensional topology that are utilized throughout the document. It serves as a reference or refresher depending on the reader's familiarity with the subject.

Chapter 3 presents the constructive proof in the smooth case. It fills a void in the current literature and anchors the abstraction of Chapter 4 to something accessible and visual.

Chapter 4 provides the algorithm. It is a precursor to an implementation of the algorithm in a low–dimensional topology software package.

Chapter 5 restates our results and delves into implications on future work. It, along with Chapter 1 and the Abstract, provide an overview of the entirety of the document.

Chapter 2

Tools of low–dimensional topology

Given a smooth, closed 3–manifold M, there are infinitely many 4–manifolds with boundary M. For example, consider $M = S^3$. Removing a 4–ball from any 4–manifold W produces a 4–manifold with S^3 boundary. Our construction begins with the 4–manifold $W = M \times [0, 1]$ which has boundary

$$\partial W = (M \times \{0\}) \cup (M \times \{1\}) = M_0 \sqcup M_1.$$

We attach stratified handles to the boundary of W away from M_0 until only M_0 remains. Handle attachment sites are obtained through a stratifying procedure in Sections 3.1 and 3.2, but only 2–handle attachment sites are immediate. The sites for 3–handles appear after considering the effect of 2–handle attachment, and the sites for 4–handles appear after considering the effect of 2– and 3–handle attachment. The remainder of this chapter sets the foundation for our analysis of the effect of handle attachments.

2.1 Handles

The concept of a stratified handle attachment needs some explanation. First, we define attachment of topological spaces, and use that language to define handle attachment. We use Gompf & Stipsicz's "4–Manifolds and Kirby Calculus" [6] as our main reference for handle attachment.

Definition 2.1.1 (Attachment). Let X and Y be topological spaces, $A \subset X$ a subspace, and $f : A \to Y$ a continuous map. We define a relation $\sim$ by putting

$f(x) \sim x$ for every x in A. Denote the quotient space $X \sqcup Y/\sim$ by $X \cup_f Y$. We call the map f the *attaching map.* We say that X is *attached* or *glued* to Y over A. A space obtained through attachment is called an *adjunction space* or *attachment space.*

Alternatively, we let A be a topological space and let $i_X : A \to X$, $i_Y : A \to Y$ be inclusions. Here, the adjunction is formed by taking $i_X(a) \sim i_Y(a)$ for every $a \in A$ and we denote the adjunction space by $X \cup_A Y$.

Definition 2.1.2 (Handle). Take $n = \lambda + \mu$ and M a smooth n–manifold with nonempty boundary ∂M. Let D^λ be the closed λ–disk and put $H^\lambda = D^\lambda \times D^\mu$. Let $\varphi : \partial D^\lambda \times D^\mu \to \partial M$ be an embedding and an attaching map between M and H^λ. The attached space H^λ is an *n–dimensional λ–handle*, abbreviated (n, λ)–*handle*, and $M \cup_\varphi H^\lambda$ is the result of an *n–dimensional λ–handle attachment*, abbreviated (n, λ)–*handle attachment.*

Let $n = \lambda + \mu$, let $H^\lambda = D^\lambda \times D^\mu$ be a (n, λ)–handle, and let $\varphi : \partial D^\lambda \times D^\mu \to \partial M$ be an attaching map from H^λ to the n–manifold M. The sphere $\partial D^\lambda \times \{0\}$ in H^λ is the *attaching sphere* of H^λ, and the sphere $\{0\} \times \partial D^\mu$ is the *belt sphere* of H^λ.

Handles H_1 and H_2 attached to M are extraneous when $(M \cup H_1) \cup H_2 \approx M$. When this happens, we say that the handles *cancel.* In the proof of Theorem 3.4.1 we attach 2–handles with the intention of canceling 1–handles.

Proposition 2.1.3 (Proposition 4.2.9 in [6])**.** A $(k-1)$–handle H^{k-1} and a k–handle H^k $(1 \leq k \leq n)$ can be canceled, provided the attaching sphere of H^k intersects the belt sphere of H^{k-1} transversely in a single point.

Handle attachment is defined for smooth manifolds, but the resulting attachment space is not a smooth manifold. Rather, the result is a manifold with corners. Some other formulations of handle attachment (e.g. [6]) implicitly smooth the corners resulting from handle attachment, so in their formulation of handle cancellation the equivalence relation is strong (i.e. $\approx$ is diffeomorphism). Instead of smoothing corners, we keep everything in the language of stratified spaces (introduced in Section 2.2). We therefore take $\approx$ to be homeomorphism for the purposes of handle cancellation.

2.2   Stratification

We use Weinberger's "The topological classification of stratified spaces" [15] as our main reference for stratified spaces.

Definition 2.2.1 (Stratification). X is a *filtered space* on a finite partially ordered indexing set S if

1. there is a closed subset X_s for each $s \in S$,

2. $s \leq s'$ implies that $X_s \subset X_{s'}$, and

3. the inclusions $X_s \hookrightarrow X_{s'}$ satisfy the homotopy lifting property.

The X_s are the *closed strata* of X, and the differences

$$X^s = X_s \setminus \bigcup_{r < s} X_r$$

are *pure strata*.

A *filtered map* between spaces filtered over the same indexing set is a continuous function $f : X \to Y$ such that $f(X_s) \subset Y_s$, and such a map is *stratified* if $f(X^s) \subset Y^s$. This leads to definitions of stratified homotopy, therefore stratified homotopy equivalence.

Immediate examples of stratified manifolds are manifolds with boundary and manifolds with corners. Many handles (e.g. $[0,1] \times [0,1]$) are manifolds with corners, and the result of a smooth handle attachment is a manifold with corners at $\varphi(\partial D^\lambda \times \partial D^\mu)$. Hence both are stratified manifolds.

A *stratified handle attachment* is a handle attachment where the handle, the manifold to which we attach the handle, and the attaching map are each stratified. The main distinctions between stratified handle attachment and handle attachment are:

1. the handle is necessarily stratified, though the stratification is not necessarily induced by the corners that occur in the standard formation of a handle as the Cartesian product of a pair of disks,

2. the manifold to which we attach the handle is necessarily stratified, and

3. the attaching map ensures that there is a coherent identification between the strata of the handle and the strata of the manifold (i.e. the stratification of the resulting attachment space is well-defined).

2.3 Handlebodies

Handlebodies are objects central to the arguments of Chapters 3 and 4. We use Gompf & Stipsicz [6] and Schleimer [12] as our main references for handlebodies. A handlebody is formed by attaching some number of (n, λ)–handles to an $(n, 0)$–handle. The name is evoked by the type of handlebody that we examine in this section: the (3,1)–handlebody.

Definition 2.3.1. A connected n–manifold M that has a handle decomposition consisting of exactly one 0–handle and g λ–handles is called an (n, λ)–*handlebody* of *genus g*.

Let V be an $(n, 1)$–handlebody of genus g. A simple closed curve in ∂V is called *essential* if it is not homotopic to a point. A simple closed curve J in ∂V that is essential in ∂V and that bounds a 2–disc in V is called a *meridian*. The properly embedded disc in V that has boundary J is called a *meridinal disc*.

The special case of the oriented genus 1 $(m, 1)$–handlebody is called a *solid torus*. More generally, any space that is homeomorphic to $S^1 \times D^{n-1}$ is called a *solid n–torus*. In our most common case of $n = 3$, we just say that $S^1 \times D^2$ is a *solid torus*. A simple closed curve J in the boundary of a solid torus that intersects a meridian at a single point is called a *longitude*. A longitude is essential in a solid torus and there are infinitely many isotopy classes of longitudes, but there is exactly one isotopy class of meridians.

We apply handlebodies to 3–manifold classification through Heegaard splittings.

Definition 2.3.2. Let U and V be 3–dimensional handlebodies of genus g and let $f : \partial U \to \partial V$ be an orientation preserving diffeomorphism. The adjunction $M = U \cup_f V$ is a *Heegaard splitting* of M, the shared boundary $H = \partial U = \partial V$ is the *Heegaard surface* of the splitting, and the shared genus of U and V is the *genus* of the splitting as well. A Heegaard splitting is also denoted by the pair (M, H).

We use the notion of equivalence between splittings from [12]: A pair of splittings (M, H) and (M, H') are *equivalent* if there is a homeomorphism $h : M \to M$ such that h is isotopic to id_M and $h|_H$ is an orientation preserving homeomorphism $H \to H'$.

Example 2.3.3. The 3–sphere S^3 has two standard Heegaard splittings. The first is the genus 0 splitting, which is realized by considering S^3 as the set of unit vectors in $\mathbb{R}^4$. Take the Heegaard surface to be the intersection of S^3 with the xyz–hyperplane
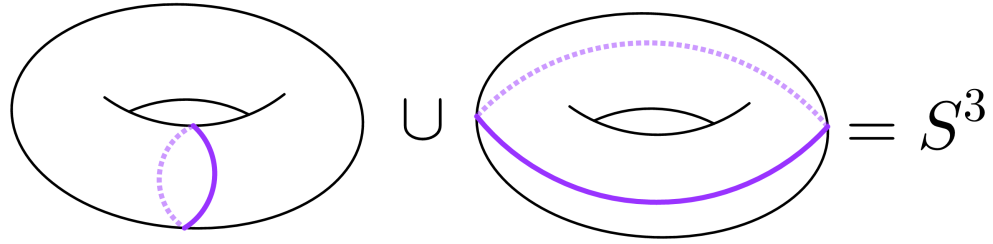
Figure 2.1: **Genus 1 Heegaard splitting of S^3.** The purple curve is essential in each solid torus pictured. In the left torus it is a meridian, on the right a longitude.

in $\mathbb{R}^4$. This is a copy of S^2 that separates S^3 into two connected components. This splitting is written (S^3, S^2)

The second is the genus 1 splitting, which is visualized using the realization of S^3 as the one–point compactification of $\mathbb{R}^3$. Take solid tori U and V and identify ∂U with ∂V by the homeomorphism that swaps a meridian with a longitude. The adjunction is S^3, and this splitting is written (S^3, T^2). Figure 2.1 displays the tori of the splitting. This description of S^3 is also obtained by examining the boundary of a 4–dimensional 2–handle $\partial(D^2 \times D^2)$.

Definition 2.3.4. Let $(M, H) = U \cup_f V$ be a Heegaard splitting of M. The connected sum $(M, H)\#(S^3, T^2)$ is called an *elementary stabilization* of M, and itself is a splitting $(M, H\#T^2)$. A Heegaard splitting (M, H) is called a *stabilization* of another splitting (M, H') if it obtained from (M, H') via a finite number of elementary stabilizations.

Consider the meridians of the solid tori in the standard genus 1 splitting of S^3. They each bound a disc in their respective handlebody, and they intersect in exactly one point. We would expect to be able to find such curves in any 3–manifold obtained as a stabilization.

Definition 2.3.5. Let $(M, H) = U \cup_f V$ be a Heegaard splitting of genus g and let α, β a pair of simple, closed, essential curves in H. Let α be a meridian of U and β be a meridian of V with associated meridinal discs D_α, D_β. If α and β intersect exactly once, then the pair (α, β) is a *meridinal pair* or *destabilizing pair* of the splitting.

To see why (α, β) would be called a destabilizing pair, remove a tubular neighbourhood of D_α from U and add it to V as a 2–handle along a tubular neighbourhood of α in H. In fact, the altered spaces U' and V' are handlebodies of genus $g - 1$

with $H' = \partial U' = \partial V'$, and (M, H) is a stabilization $(M, H') \# (S^3, T^2)$. We say that (M, H') is a *destabilization* of (M, H) over (α, β). Note that when we consider β to be the belt sphere of a 1–handle and α to be the attaching sphere of a 2–handle, a destabilization is also a handle cancellation.

Chapter 3

Construction for smooth manifolds

We prove that every smooth, closed, orientable 3–manifold is the boundary of some 4–manifold. We do so by explicitly constructing such a 4–manifold from a given 3–manifold. This construction is mirrored in Chapter 4 where we prove the same for a given closed, orientable 3–manifold triangulation and provide an algorithm.

Let M be a smooth, closed, orientable 3–manifold and take $W = M \times [0,1]$. Then W is a 4–manifold with boundary

$$\partial W = (M \times \{0\}) \cup (M \times \{1\}) = M_0 \cup M_1.$$

We construct a manifold with only one boundary component from W by attaching 4–dimensional 2–, 3–, and 4–handles to W over the part of its boundary away from M_0. We start by attaching 2–handles to W over M_1 to produce a 4–manifold W' with boundary $M_0 \sqcup M_1'$, where $M_1' = \partial W' \setminus M_0$ and is described via surgery on M_1. We then attach 3–handles to W' over M_1' to produce a 4–manifold W'' with boundary $M_0 \sqcup M_1''$. As before, $M_1'' = \partial W'' \setminus M_0$ and M_1'' is described via surgery on M_1'. At this point in the construction, M_1'' is the disjoint union of a finite number of copies of S^3. We attach 4–handles to W'' over M_1'' to produce a 4–manifold whose boundary is exactly M_0.

Instructions for handle attachment come from defining a projection $f : M_1 \to \mathbb{R}^2$ that induces a stratification of $M_1 \subset \partial W$.

We call a closed 3–dimensional stratum of M_1 a *block*, and we impose conditions on f to ensure that every block can be classified up to *stratified homeomorphism*. We say that X, Y are *stratified homeomorphic* if X, Y are stratified spaces and there exists a homeomorphism $f : X \to Y$ such that f and f^{-1} are each stratified maps.

The blocks of M_1 are described below:

Face block: An attachment neighbourhood for a stratified 2–handle. Each face block is stratified-homeomorphic to $S^1 \times G_n$, the product of the circle with an n-gon for some n.

Edge block: A partial attachment neighbourhood for a stratified 3–handle. Each edge block is stratified-homeomorphic to one of $D^2 \times [0,1]$, $A \times [0,1]$, or $P \times [0,1]$, where A is the annulus $S^1 \times [0,1]$ and P is a pair-of-pants surface. Attachment of stratified (4,2)–handles over our face blocks "fill in" the annular boundary components of edge blocks, forming full attachment neighbourhoods for stratified 3–handles.

Vertex block: A partial attachment neighbourhood for a stratified 4–handle. Each vertex block is homeomorphic to a (3,1)-handlebody of genus at most 3. When stratified (4,2)– and (4,3)–handles are attached to W, the genus of each vertex block is reduced until the remaining boundary of W consists of M_0 union a collection of stratified 3–spheres. The 3–spheres are then coned away.

The remainder of this chapter is spent ensuring that such a stratification can be achieved for any smooth, orientable, closed 3–manifold, detailing how the stratification is induced, proving that the attachment of stratified (4,2)– and (4,3)–handles has the previously stated effects, and discussing the resulting 4–manifold.

3.1 Projections from 3–manifolds to $\mathbb{R}^2$

Our stratification of M is induced by a decomposition of the plane, itself induced by the singular values of a smooth map $M \to \mathbb{R}^2$. To prove that a stratification suitable for our construction exists for any smooth orientable 3–manifold, we show first that an inducing decomposition of $\mathbb{R}^2$ exists. To prove that such a decomposition of $\mathbb{R}^2$ exists, we present the properties of $f : M \to \mathbb{R}^2$ required to induce the decomposition, and argue why a map possessing such properties exists for any smooth, orientable 3–manifold.

Let $f : M \to \mathbb{R}^2$ be a smooth map, let df be the differential of f, and let $S_r(f)$ be the set of points in M such that df has rank r. Then we require that the following be true of f:

1. $S_0(f)$ is empty.

2. $S_1(f)$ consists of smooth non-intersecting curves. We call these the *fold curves* of f.

3. The set of points where $f|_{S_1(f)}$ has zero differential is empty.

4. If $p \in S_1(f)$ then there exist coordinates (u, z_1, z_2) centred at p and (x, y) centred at $f(p)$ such that f takes the form of either

   (a) $(x, y) = (u, \pm(z_1^2 + z_2^2))$, or

   (b) $(x, y) = (u, \pm(z_1^2 - z_2^2))$

   in a neighbourhood of p. If f takes the form of (4a) then we further classify p as a *definite fold*, and if f takes the form of (4b) then p is an *indefinite fold*.

5. Let $\gamma_i, \gamma_j, \gamma_k \in S_1(f)$ be fold curves. Then each of $f(\gamma_i)$, $f(\gamma_j)$, $f(\gamma_k)$ is a submanifold of $\mathbb{R}^2$ such that

   (a) $f(\gamma_i)$ and $f(\gamma_j)$ intersect transversely,

   (b) $f(\gamma_i) \cap f(\gamma_j) \cap f(\gamma_k)$ is empty (i.e. there are no triple-intersections), and

   (c) self-intersections of $f(\gamma_i)$ are transverse

6. The set of singular values of f in the plane is connected

7. The image of M through f is bounded in the plane.

We call these the *stratification conditions* on f, and we call a map satisfying the stratification conditions a *stratifying map*. The existence of smooth maps satisfying conditions 1–4 is discussed in [8], 5 & 6 can be guaranteed by a suitable modification of a map that satisfies 1–4, and condition 7 is always satisfied because the image of a compact set through a continuous map is compact. A smooth map satisfying conditions 1–4 can be smoothly perturbed inside of a tubular neighbourhood of $S_1(f)$ to satisfy condition 5. A map satisfying conditions 1–5 is homotopic to one that also satisfies condition 6, but the homotopy passes through functions that have cusps, i.e. that do not meet condition 1.

Let K and L be folds in M such that $f(K)$ and $f(L)$ belong to disjoint connected components of $f(S(f))$ in the plane. We create a definite fold and an indefinite fold that meet at a pair of cusp points (As in Lemma 3.1 of [10]). This is a 'matching

pair' of cusps (due to results in section 4 of [8]), and we connect that matching pair of cusps using an arc that links each of K and L in M. A band operation (Lemma 3.7 of [10]) on that arc then eliminates the cusps and leaves behind two folds, one definite and one indefinite, whose images in the plane necessarily intersect each of $f(K)$ and $f(L)$, and each of the first four conditions are still satisfied by these moves.

To see the main implication of condition 6, let $f : M \to \mathbb{R}^2$ be a stratifying map and let $X_f = f(S(f))$, the set of singular values of f. We first consider $f(M) \setminus X_f$. Because X_f is a connected collection of arcs in the plane that intersect only transversely, $f(M) \setminus X_f$ is a collection of connected regions in the plane, each of which consists entirely of regular values. Stratification condition 6 guarantees that each of these regions is simply connected — the boundary components of these regions are formed by the singular values of f in the plane, and different boundary components are necessarily disjoint. The sixth stratification condition does not restrict the class of maps we consider because, as we have just seen, a map satisfying the first five stratification conditions is smoothly homotopic to one satisfying the sixth.

3.2 Stratifying $\mathbb{R}^2$

Let $f : M \to \mathbb{R}^2$ be a stratifying map with singular values X_f. We fit closed neighbourhoods (*sleeves*) around the singular values of f and classify these sleeves by the maximum codimension (with respect to $\mathbb{R}^2$) of singular values they contain. Because X_f consists of codimension 1 and codimension 2 singular values (arcs and arc-crossings respectively) in the plane and the endpoints of each arc of codimension 1 singular values is a pair of (not necessarily distinct) codimension 2 singular values, we stratify $\mathbb{R}^2$ into face regions that contain no singular values, edge regions that contain only codimension 1 singular values, and vertex regions, each of which contain exactly 1 codimension 2 singular value.

The naming convention is due to the natural structure X_f has of an embedded planar graph whose vertices are codimension 2 singular values and whose edges are arcs of codimension 1 singular values. We refer to the codimension 2 singularities as the vertices of X_f, the arcs of codimension 1 singularities as the edges of X_f, and the regions of regular values comprising $f(M) \setminus X_f$ as the faces of X_f. Figures 3.1-3.4 are used to illustrate the stratification resulting from sleeve-fitting.

We begin by fitting sleeves around codimension 2 singular values as in Figure 3.2. These sleeves are each boundary-stratified 2–discs with exactly eight 1–dimensional
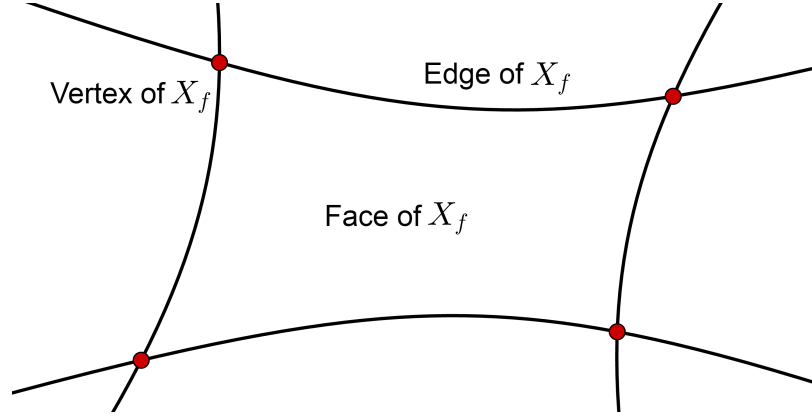
Figure 3.1: **Singular values of f.** Vertices are arc crossings, edges are arcs, and connected components of $f(M) \setminus X_f$ are faces.
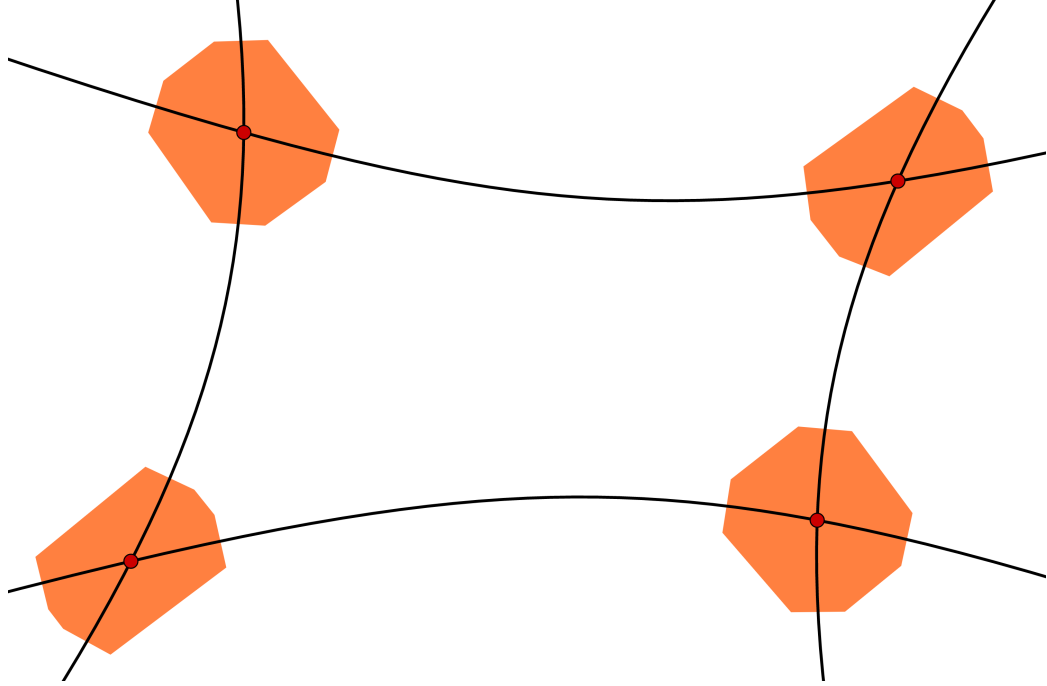
Figure 3.2: **Forming vertex regions.** Octagonal sleeves are fit around the vertices of X_f to form vertex regions, shaded orange. Vertex regions are fit around vertices so that each 1-strata either consists entirely of regular values or contains exactly one singular value: its intersection with an edge of X_f. Furthermore, this classification is an alternating pattern around the boundary of a vertex sleeve.

boundary strata (i.e. octagons). Following the notation patterns already present in this document, we call the k–dimensional strata of a stratified manifold the k–*strata* of that manifold. If x is a codimension 2 singular value then x is the result of an arc

crossing, and a small neighbourhood around an arc crossing is divided into four regions of regular values. The octagon around x is fit so that its 1–strata alternate between being fully contained in a region of regular values and orthogonally intersecting one of the arcs of singular values that creates x, as depicted by the example fitting in Figure 3.2.

The closed octagons form the vertex regions of the stratification of $\mathbb{R}^2$. The octagons are chosen to be small enough that no two vertex regions overlap and such that the 1–strata that intersect arcs of codimension 1 singular values are all the same length.
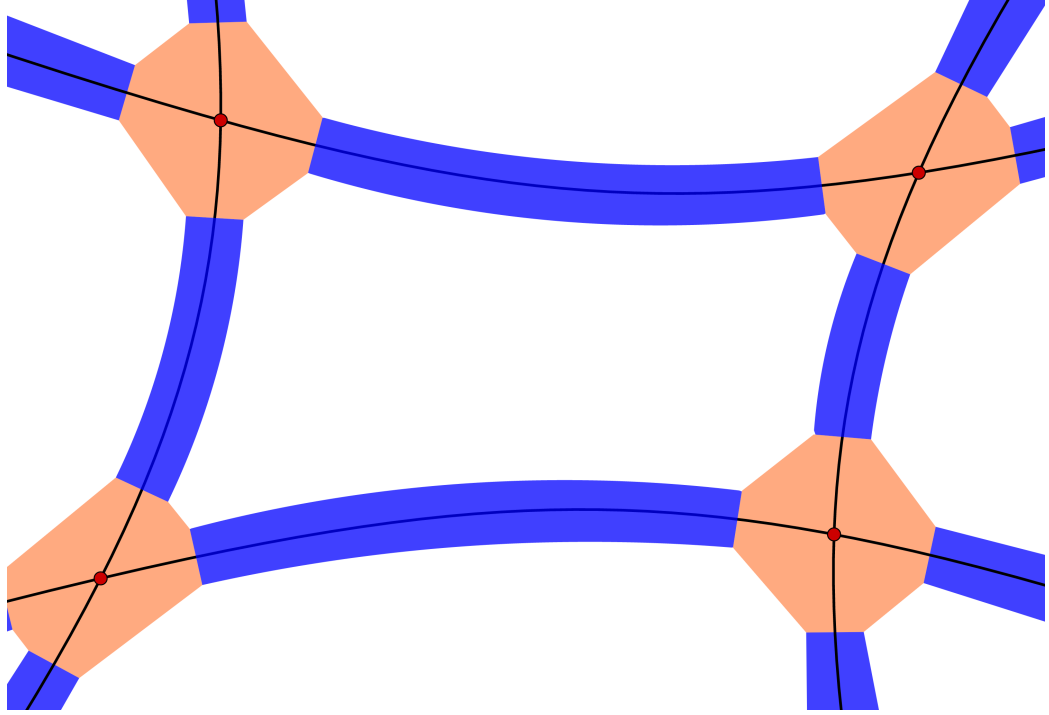
Figure 3.3: **Forming edge regions.** Vertex region corners are connected to fit sleeves around arcs of codimension 1 singular values to form edge regions. New edge regions are shaded blue.

Let γ be an edge of X_f with endpoints a pair of vertices. γ orthogonally intersects one 1–strata from each of the octagonal vertex regions fit around its endpoints, and we use these 1–strata to form the edge region associated to γ by connecting the 0–strata boundaries of the 1–strata to one another using a pair of arcs parallel to γ, as illustrated in the example edge region fitting of Figure 3.3.

We form the boundary of the edge region associated with γ as the union of:

1. the arcs parallel to γ connecting vertex region 0–strata, and

2. the vertex region 1–strata that intersect γ

This union is a simple closed curve J. The component of $\mathbb{R}^2 \setminus J$ that contains no vertices of X_f is a boundary stratified 2–disc that shares two of its four boundary 1–strata with the vertex regions on either end of γ. This boundary stratified 2–disc is then the edge region of the stratification of $\mathbb{R}^2$ associated with γ.
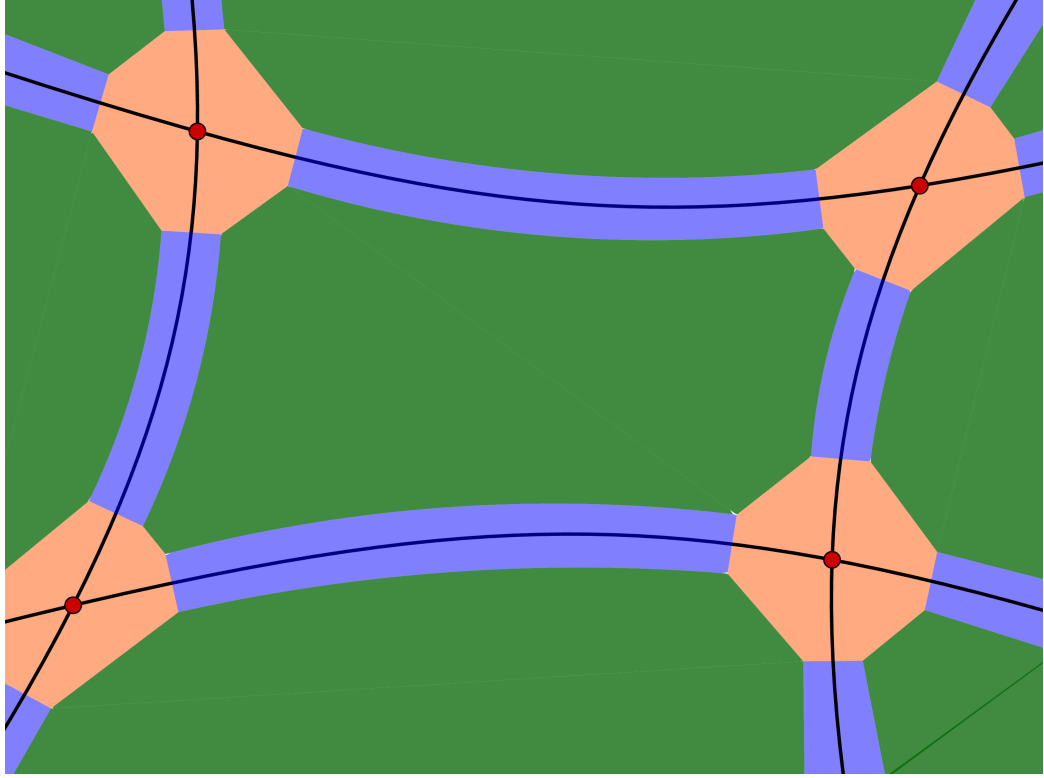
Figure 3.4: **Forming face regions.** All remaining regions contain no singular values, and we take these to be the face regions. New face regions are shaded green.

Removing from $f(M)$ all vertex and edge regions, we are left with a collection of connected regions in the plane, each of which is a deformation retract of a face of X_f. We take the closures of these to be the face regions of the stratification of $\mathbb{R}^2$. The boundary of each face region is an alternating collection of boundary 1–strata from edge regions and boundary 1–strata from vertex regions. See Figure 3.4 for an example fitting.

With all of the regions defined, we can describe precisely how f stratifies $\mathbb{R}^2$. The stratification of $\mathbb{R}^2$ is a stratification into subsets $R_{(i,j)}$ where i, j are integers. Subset indexing is defined so that a subset $R_{(i,j)}$ is an i–dimensional submanifold of $\mathbb{R}^2$, thus $R_{(i,j)} \nleq R_{(k,l)}$ if $i \nleq k$. The first collection of subsets used to filter $\mathbb{R}^2$ are the

0–strata of the octagonal vertex sleeves. We assign to these subsets the indices $(0, i)$ for $i = 1, \ldots, N_0$, where N_0 is the number of 0–strata. Our 0–strata are disjoint, so for any i, j with $i \neq j$, $R_{(0,i)}$ is not contained in $R_{(0,j)}$, hence $(0, i) \not\leq (0, j)$.

The boundary 1–strata connect the $(0, i)$–level strata. These 1–strata are indexed by $(1, j)$ for $j = 1, \ldots, N_1$, where N_1 is the number of arcs. The boundary points of 1–strata are 0–strata and are subsets of the filtration indexed by the $(0, i)$ indices, so $(0, i) \leq (1, j)$ if and only if $R_{(0,i)}$ is one of the boundary points of $R_{(1,j)}$. Our 1–strata intersect only at their boundary points, so $(1, j) \not\leq (1, k)$ for any j, k.

The regions themselves are indexed by $(2, k)$ for $k = 1, \ldots, N_2$, where N_2 is the number of regions. These indices work similarly to the 1–strata indices. The boundary of a region consists of 0– and 1–strata, so $(n, i) \leq (2, k)$ if and only if $R_{(n,i)}$ is contained in the boundary of $R_{(2,k)}$.

With $\mathbb{R}^2$ stratified, we move onto a stratification of M. This stratification is induced by the preimages of the strata of $\mathbb{R}^2$.

3.3 Stratifying M

Stratifying $\mathbb{R}^2$ via the singular values of f also induces a stratification of M by considering the fibers of f above the stratifying regions. The interiors of face regions have preimage through f a disjoint collection of face blocks, the interiors of edge regions have preimage of edge blocks, and of vertex regions, vertex blocks.

To understand the structure of face, edge, and vertex blocks we investigate the preimages of regular and singular values of f in the plane.

Definition 3.3.1. Because M is closed, f is proper. Thus, for any point q in $f(M)$, a fiber of f above q (i.e. a connected component of $f^{-1}(q)$) is either a closed 1–manifold (i.e. S^1) or contains a critical point of f.

We define a *singular fiber* to be a fiber that contains a critical point of f, and a *regular fiber* to be a fiber consisting entirely of regular points.

The subsets used to stratify M are the fibers of f that lie above the individual strata of our $\mathbb{R}^2$ stratification. Because the $(0, \cdot)$–strata are regular values, their fibers are regular, hence a finite collection of disjointly embedded circles in M. We take these circles as the first collection of subsets that filter M, and assign to them the indices $(1, i)$ for $i = 1, \ldots, N_1$, where N_1 is the number of circles. These circles are disjoint, so $(1, i) \not\leq (1, j)$ for any i, j.

The $(1, \cdot)$–strata of the $\mathbb{R}^2$ stratification connect the $(0, \cdot)$–strata of the $\mathbb{R}^2$ strat-
ification and either consist entirely of regular values or contain exactly one singular
value. As pictured in Figure 3.4, a $(1, \cdot)$–strata contains exactly one singular value
precisely when it is the shared boundary of a vertex region and an edge region. When
a $(1, \cdot)$–strata contains exactly one singular value, exactly one fiber above that value
is a singular fiber, with the rest regular fibers. A $(1, \cdot)$–strata is diffeomorphic to
the unit interval and f is a smooth submersion between smooth manifolds, so a fiber
above a $(1, \cdot)$–strata is a surface whose boundary circles are the fibers above the
strata's endpoints. When the fiber is regular, the surface is diffeomorphic to an an-
nulus $S^1 \times [0, 1]$. When the fiber is singular, the surface classification depends on the
type of singularity. Theorem 3.3.2 and Figure 3.5 show that the fiber containing the
singularity either has the structure of a figure-of-eight (when the singularity is part
of an indefinite fold) or is a single point (when the singularity is part of a definite
fold), hence the singular fiber above the arc is diffeomorphic to either a 2–disk or a
pair-of-pants.

Theorem 3.3.2 refers to a *stable map*, and we'll denote the set of smooth stable
maps $X \to Y$ by $Stab(X, Y)$. When X is a smooth, closed, orientable 3–manifold
and Y is the plane, $Stab(X, Y)$ consists of all maps $X \to Y$ satisfying the first five
stratification conditions. The last stratification condition is trivially satisfied because
X is closed, hence the set of stratifying maps $X \to Y$ is the subset of $Stab(X, Y)$
consisting of maps f such that $f(S(f))$ is connected.

Theorem 3.3.2 (Adapted Theorem 3.15 in Saeki [11])**.** Let $f : M \to N$ be a proper
C^∞ stable map of an orientable 3–manifold M into a surface N. Then, every singular
fiber of f is equivalent to the disjoint union of:

1. one of the fibers in Figure 3.5, and

2. the disjoint union of a finite number of copies of S^1.

Furthermore, no two fibers in the list are equivalent to each other even after taking
the union with regular circle components.

The surface fibers above the $(1, \cdot)$–strata are the second collection of subsets that
filter M, and they are assigned the indices $(2, j)$ for $j = 1, \ldots, N_2$, where N_2 is the
number of surfaces. The boundary circles of the surfaces are each subsets of the
filtration, indexed by the $(1, i)$ indices, so $(1, i) \leq (2, j)$ if and only if $M_{(1,i)}$ is one of

$\kappa = 1:$

$\kappa = 2:$
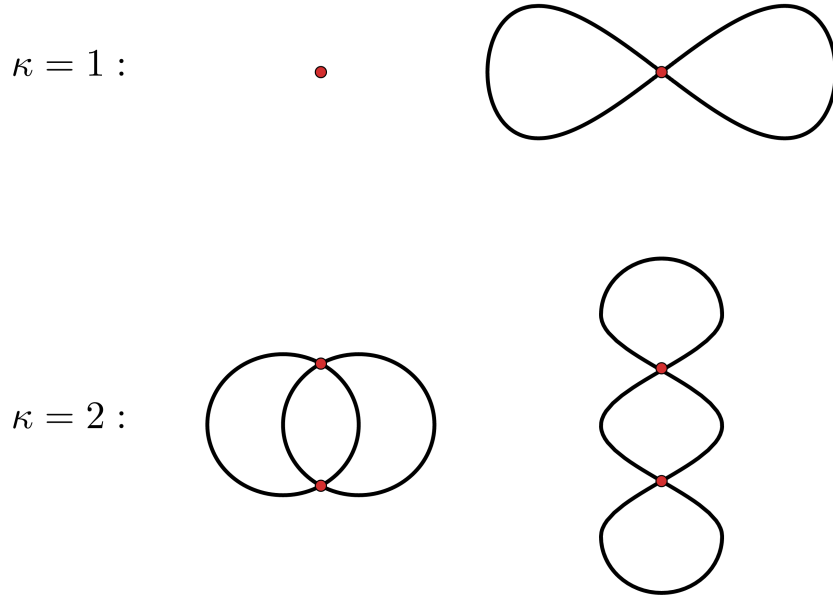
Figure 3.5: **Connected singular fibers.** List of connected singular fibers of proper C^∞ stable maps of orientable 3–manifolds into surfaces. κ is the codimension of the singularity in the surface. The singular fiber above a codimension 2 singular value may be disconnected, in which case the fiber is the disjoint union of a pair of singular fibers from $\kappa = 1$.

the boundary components of $M_{(2,j)}$. These surfaces intersect one another only when they share a boundary circle, so $(2, j) \not\leq (2, k)$ for any j, k.

There are three types of region in the decomposition: face, edge, and vertex. Regardless of the type of region, they are indexed in our filtration similarly to the edges. A fiber above a region is a 3–manifold with corners formed by the $(1, i)$- and $(2, j)$-level strata, and fibers are disjoint away from their boundaries. We therefore index fibers above regions with the indices $(3, k)$ for $k = 1, \ldots, N_3$ where N_3 is the total number of fibers above regions, put $(n, i) \leq (3, k)$ if and only if $M_{(n,i)}$ is contained in the boundary of $M_{(3,k)}$.

Recall that we call a closed 3–dimensional stratum of M a *block*. At the beginning of this chapter we laid out the structure of the blocks that we expect to find inside of M and, with stratification complete, we are now able to investigate these structures and determine how they are formed. Blocks are categorized by the $\mathbb{R}^2$-stratification regions they project to: as face, edge, or vertex blocks. This classification determines the possible singularities that we can find inside of a block. We first restate the definitions of the various blocks and include partial justifications based on the singularities of M.

In Theorem 3.3.4 we prove that the stratification conditions impose this structure on the blocks of M.

Face block: Let B be a face block that fibers over the face region F. Then B is stratified–homeomorphic to $S^1 \times F$.

Edge block: Let B be an edge block that fibers over the edge region E. Let A be the annulus $S^1 \times [0,1]$ and P the pair-of pants surface (i.e. D^2 minus a pair of disjoint open balls). If B is a regular fiber over E then B is stratified–homeomorphic to $S^1 \times E$, hence also stratified–homeomorphic to $A \times [0,1]$. Otherwise, B is a singular fiber over E and contains part of a definite or indefinite fold. In this case we call B a *definite* or *indefinite edge block*. A definite edge block is stratified–homeomorphic to $D^2 \times [0,1]$ and an indefinite edge block is stratified–homeomorphic to $P \times [0,1]$.

Vertex block: Let B be a vertex block that fibers over the vertex region V. If B is a regular fiber then it is homeomorphic to $S^1 \times V$, therefore homeomorphic to a (3,1)–handlebody of genus 1. Otherwise, we see from Figure 3.5 that the singular fiber above the codimension 2 singularity contained in V is either connected or disconnected. If the singular fiber is disconnected then there is a pair of disjoint vertex blocks that each contain one of the singular fibers, hence part of a definite or indefinite fold. We therefore classify these blocks as *definite* or *indefinite vertex blocks*. If the singular fiber is connected, then the block containing it is an *interactive vertex block*. A definite (resp. indefinite) vertex block extends and connects definite (resp. indefinite) edge blocks, and is homeomorphic to a (3,1)–handlebody of genus 0 (resp. 2). An interactive vertex block is homeomorphic to a (3,1)–handlebody of genus 3.

Remark 3.3.3. The structures of the blocks are roughly disk bundles over a representative fiber for the given region or, equivalently, regular neighbourhoods of that fiber. For a block that is a regular fiber, the representative is a circle. For a definite or indefinite block, the representative is the singular fiber containing a definite or indefinite fold, and for an interactive block the representative fiber is the singular fiber above the codimension 2 singular value.

Theorem 3.3.4. Let M be a smooth, closed, orientable 3–manifold, let $f : M \to \mathbb{R}^2$ be a stratifying map, suppose $\mathbb{R}^2$ has been decomposed as in Section 3.2 and M has

been stratified as in this section. Let B be a block of M. Then B is a face, edge, or vertex block if $f(B)$ is a face, edge, or vertex region respectively.

Proof. We split the proof into three parts. The first part proves that if a block B is a regular fiber over the region R then B is stratified–homeomorphic to $S^1 \times R$. In the second part, we prove that definite and indefinite blocks are stratified–homeomorphic to $D^2 \times [0,1]$ or to $P \times [0,1]$ respectively. In the final part we discuss interactive vertex blocks, and show that they are homeomorphic to (3,1)–handlebodies of genus 3. Figures 3.6-3.15 illustrate block structures.

Part 1: Let B be a block over the region R, and suppose B consists entirely of regular fibers over R. Then $(B, R, f|_B, S^1)$ has the structure of a circle bundle over R. A fiber bundle over a contractible space is trivial, so B is homeomorphic to $S^1 \times R$. Furthermore, this homeomorphism is stratified by ensuring the strata of B are mapped to the strata of $S^1 \times R$, where the stratification of $S^1 \times R$ is defined by the manifold with corners structure induced by the product topology.
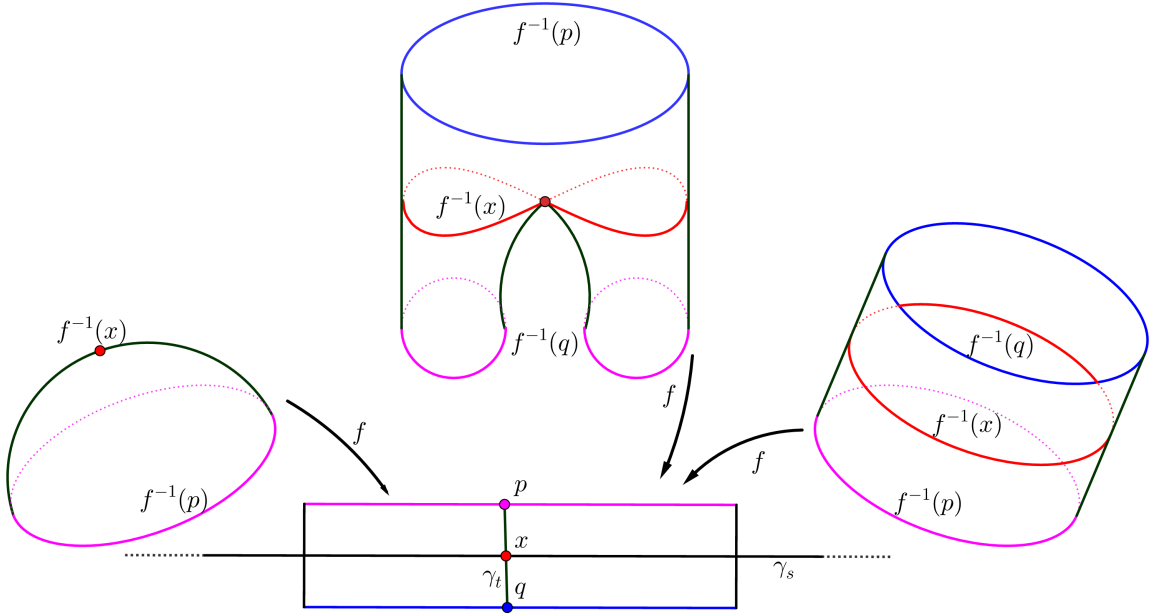
Figure 3.6: **Surfaces over codimension 1 singularities.** γ_s is an arc of singular values and γ_t is an arc with endpoints $\partial \gamma_t = \{p, q\}$ that intersects γ_s transversely at $x = \gamma_s \cap \gamma_t$. The three surfaces shown are the three possible cross-sectional surfaces that can project through f over γ_t.

Part 2: Let B be a definite or indefinite block over the region R. R is a subset of the plane homeomorphic to D^2 with an arc $\gamma_s \subset X_f$ of singular values running from
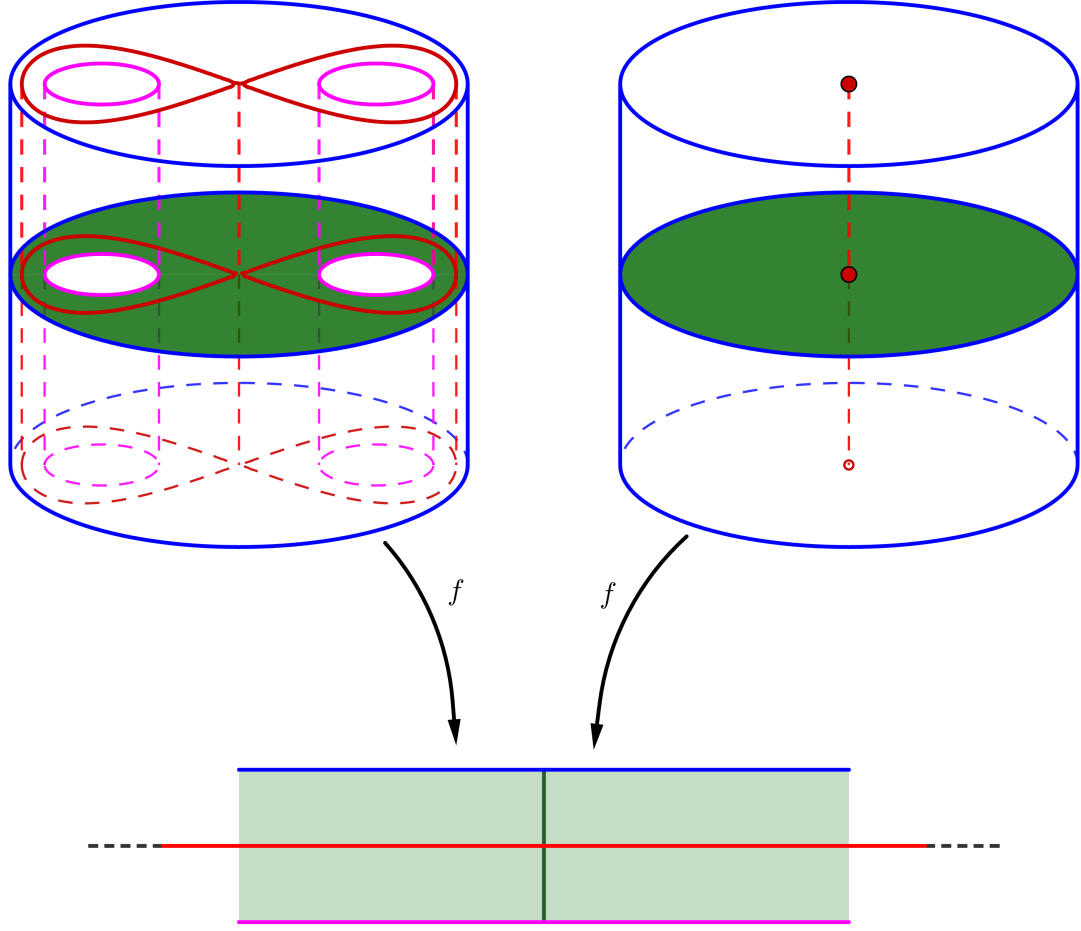
Figure 3.7: **Definite and indefinite blocks.** The blocks containing sections of definite and indefinite folds that project over codimension 1 singular values. These are found as singular fibers over edge and vertex regions.

one of its edges to another. Let γ_t be a second simple arc that crosses γ_s transversely, and consider the cross-sectional surface obtained by $f^{-1}(\gamma_t)$. Figure 3.6 illustrates the possible surfaces containing the singular fiber over $x = \gamma_s \cap \gamma_t$.

This cross section is general, so we fit a tubular neighbourhood $\nu(\gamma_s)$ about γ_s in R to obtain a bundle structure for $f^{-1}(\nu(\gamma_s))$ whose fiber is one of the cross-sectional surfaces (a disk or a pair-of-pants) and whose base is the arc γ_s, i.e. an interval. The interval is contractible, so $f^{-1}(\nu(\gamma_s))$ is homeomorphic to $\Sigma \times [0, 1]$ for Σ a disk or a pair-of-pants surface. Away from $\nu(\gamma_s)$, R consists entirely of regular values so we obtain solid tori (cf. Part 1) that extend the $\Sigma \times [0, 1]$ structure as seen in Figure 3.7.

As with Part 1, the homeomorphism described is stratified by ensuring the strata

of B are mapped to the strata of $\Sigma \times [0, 1]$, where the stratification of $\Sigma \times [0, 1]$ is defined by the manifold with corners structure induced by the product topology.

Part 3: Let B be an interactive block over the region R. Interactive blocks occur over octagonal vertex regions where the singular fiber above the region's codimension 2 singularity is connected, so we investigate these fibers. The codimension 2 singular value lies at the intersection of a pair of arcs of codimension 1 singular values. Call the arcs γ_1 and γ_2, let $x = \gamma_1 \cap \gamma_2$, and denote the interactive singular fiber over x by $B_x = B \cap f^{-1}(x) = \{b \in B \mid f(b) = x\}$. Our method of investigation begins by examining the possible resolutions of B_x and combining those resolutions to form a genus 3 surface.

Figure 3.8 demonstrates resolutions of the singular points of B_x when B_x has the first interactive singular fiber form presented in Figure 3.5. We first note that all of the displayed fibers have inherited an orientation from M. This forces fiber resolution to be unambiguous, and allows us to identify fibers when forming the surface shown in Figure 3.9.
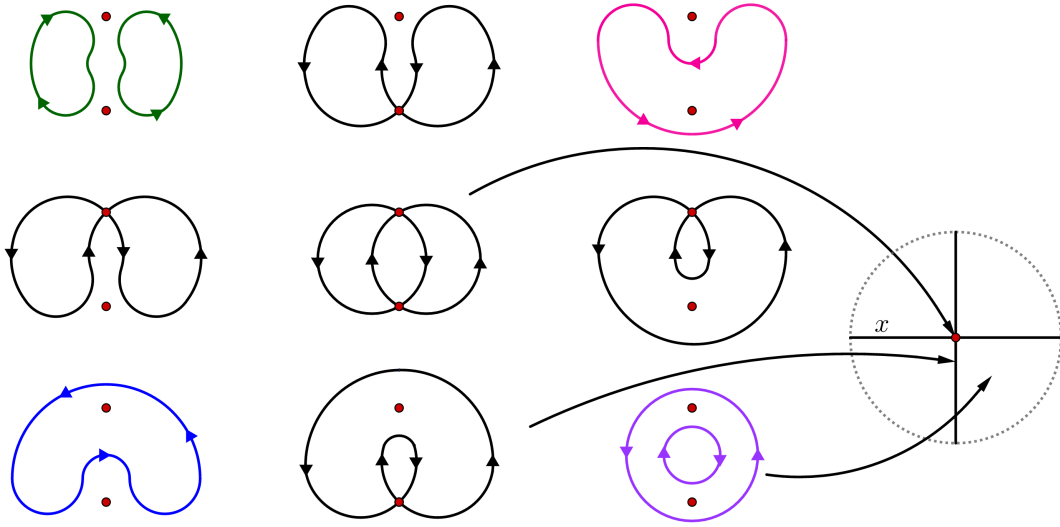
Figure 3.8: **Resolutions of the singular points in the first interactive fiber.** The singular fiber inside of B_x and its possible resolutions over nearby codimension 1 singular values and regular values. The fibers inherit orientation from M, and this illustration is presented without loss of generality. This figure is modeled after Figure 18 from [4].

We form the surface shown in Figure 3.9 by gluing together surfaces that project over simple arcs transversing the codimension 1 singular values. Gluing is performed
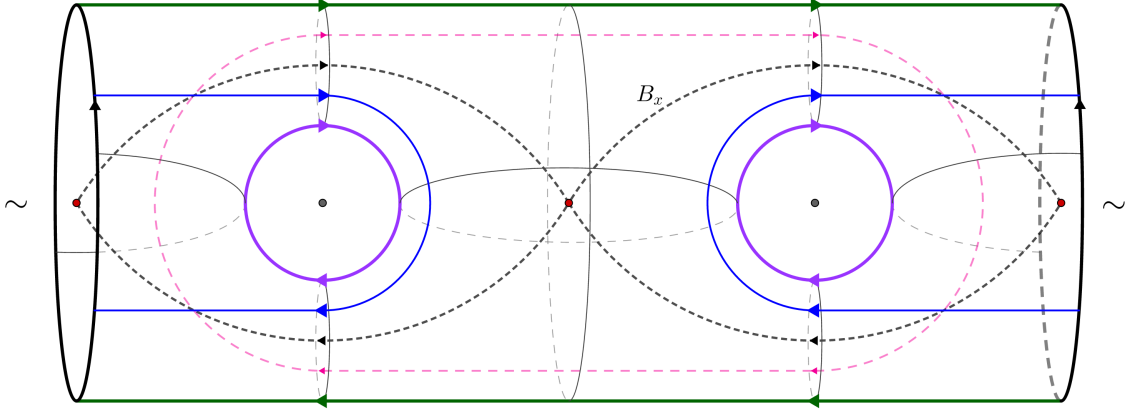
Figure 3.9: **Surface Σ near the first interactive fiber that projects over $\partial\bar{\nu}(x)$.** The surface and B_x are presented as embedded in S^3, where $H(B_x)$ is the genus-3 (3,1)–handlebody on the 'inside' of Σ in S^3.

over the boundary circles of these surfaces, and is prescribed by the resolutions in Figure 3.8. The transverse preimage containing the left column of fibers in Figure 3.8 is a pair of pants with two green 'cuffs' (top left) and a blue 'waist' (bottom left). The preimage containing the top row is a pair of pants with two green cuffs (top left) and a pink waist (top right). The first gluing that helps realize the surface in Figure 3.9 is of the 'left' transverse preimage surface with the 'top' transverse preimage surface over their shared green cuffs. The surfaces recovered as transversal preimages are then:

Left: a pair of pants with blue waist and green cuffs

Top: a pair of pants with pink waist and green cuffs

Right: a pair of pants with pink waist and purple cuffs

Bottom: a pair of pants with blue waist and purple cuffs

The surface Σ in Figure 3.9 is the boundary of $H(B_x)$, a regular neighbourhood of B_x in M, i.e. a genus-3 (3,1)–handlebody inside of M. $H(B_x)$ projects through f over $\bar{\nu}(x)$, a closed tubular neighbourhood of x, and Σ projects over $\partial(\bar{\nu}(x))$.

Figure 3.9 presents Σ and B_x as objects embedded in S^3, where Σ bounds genus-3 (3-1)–handlebodies on both sides. We take the 'inside' component of $S^3 \setminus \Sigma$ (i.e. the component containing B_x) to be $H(B_x)$.

Outside of $\bar{\nu}(x)$ we use the investigations from Parts 1 and 2 of this proof. The rest of R, $f^{-1}(R \setminus \bar{\nu}(x))$, has the structure of a Σ-bundle over the interval, and the bundle extends $H(B_x)$ to the boundary of R, preserving the structure as a genus-3 (3,1)–handlebody. We conclude that B is homeomorphic to a genus-3 (3,1)–handlebody.
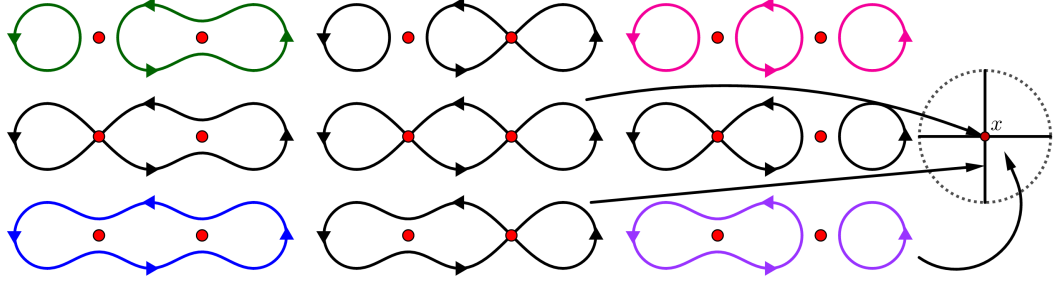
Figure 3.10: **Resolutions of the singular points in the second interactive fiber.** The singular fiber inside of B_x and its possible resolutions over nearby codimension 1 singular values and regular values. The fibers inherit orientation from M, and this illustration is presented without loss of generality. This figure is modeled after Figure 16 from [4].
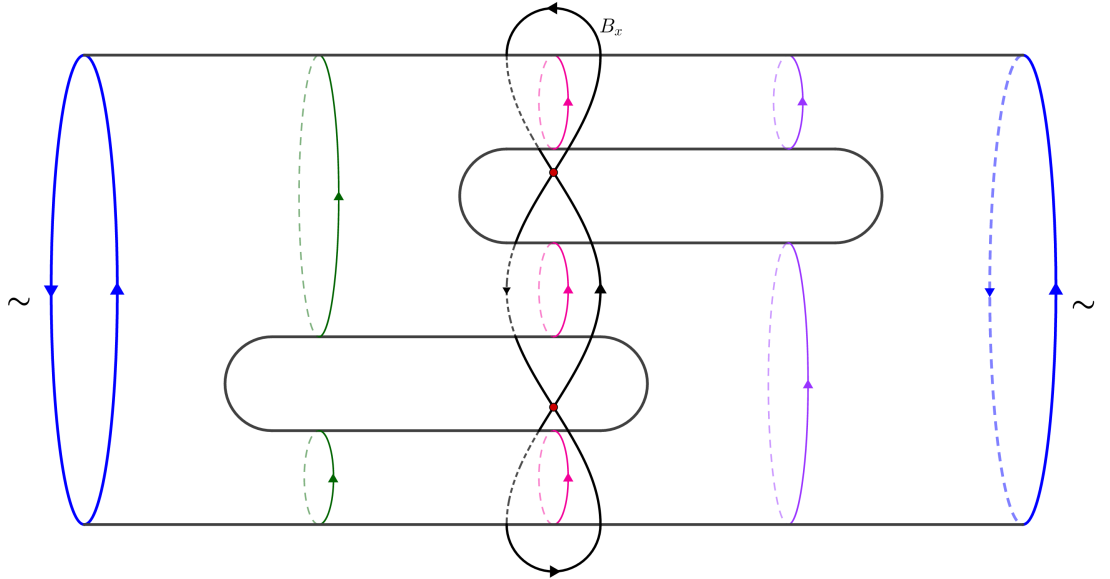
Figure 3.11: **Surface Σ near the second interactive fiber that projects over $\partial\bar{\nu}(x)$.** The surface and B_x are presented as embedded in S^3, where $H(B_x)$ is the genus-3 (3,1)–handlebody on the 'outside' of Σ in S^3.

An identical argument is made when B_x has the second interactive singular fiber

form, using Figures 3.10 and 3.11 in place of Figures 3.8 and 3.9 respectively. In this case the surfaces recovered as transversal preimages are:

Left: a pair of pants with blue waist and green cuffs

Top: the disjoint union of a pair of pants with green waist and pink cuffs with an annulus with one green boundary circle and one pink boundary component

Right: the disjoint union of a pair of pants with purple waist and pink cuffs with an annulus with one purple boundary circle and one pink boundary component

Bottom: a pair of pants with blue waist and purple cuffs

$\square$

A smooth map f satisfying the stratification conditions of Section 3.1 induces a decomposition on $\mathbb{R}^2$ and a stratification of M. It is important to note here that the restrictions on f can induce a wide variety of possible stratifications of M, highlighting the variability of the resulting 4–manifold. We end this section with a lemma that guarantees the stratified 2–handle attachments of the next section can be made over our face blocks in any order, hence we can assume all attachments occur simultaneously.

Lemma 3.3.5. Let M be a 3–manifold with stratification induced as in Theorem 3.3.4. Then blocks of the same type (i.e. face, edge, vertex) are disjoint.

Proof. The fibers above a given region are disjoint, so the blocks above that region are disjoint. Regions of the same type are disjoint, hence blocks that are fibers above differing regions are also disjoint. $\square$

3.4 Attach Handles

Stratifying M allows the definition of attachment neighbourhoods for stratified 2–, 3–, and 4–handles in $W = M \times [0, 1]$. A 4–dimensional 2–handle is attached over a closed solid torus embedded in the boundary of a 4–manifold, so attachment neighbourhoods for our stratified 2–handles are straightforward: they are the face blocks of M. We alter the boundary of W by attaching handles, so the attachment neighbourhoods for 3–handles (4–handles, resp.) must be found after 2–handles (3–handles, resp.) are attached. For a 3–handle, an attachment neighbourhood consists of the union of an

edge block with some strata introduced by 2–handle attachment. For a 4–handle, an attachment neighbourhood consists of the union of an edge block with some strata introduced by 2– and 3–handle attachments. We investigate the consequences of handle attachment by comparing the boundary of the initial manifold with the boundary of the manifold resulting from handle attachment, and use a precisely defined handle structure to focus the investigation. Our first step is to precisely define the structure of the stratified 2–handles that we are attaching.

3.4.1   2–handles

Let B be a face block of M_1. By Theorem 3.3.4, B is a closed solid torus that is stratified-homeomorphic to $S^1 \times G_n$, where G_n is an n–gon for some n. Consider an unknotted embedding of B in S^3. The complement of the interior of B is another closed solid torus B'. The tori B and B' are depicted as cylinders with top and bottom identified in Figure 3.12.

We stratify B' as follows. First include the shared stratified boundary of B. Next, introduce meridinal disks of B' that are bounded by the $(1, i)$–indexed strata in B, i.e. the boundary curves in B corresponding to $S^1 \times c_m$ where c_m is a corner of G_n, $m = 1, \ldots, n$. Finally, add the homeomorphic 3–disks of B' whose boundaries consist of one longitudinal annulus of B along with the two meridinal disks in B' that are bounded by the annulus's circular boundary components. The filtration of B' is created identically to that of the original face blocks, using inclusion as a partial ordering and indexing a stratum by its dimension as a submanifold of B'. Figure 3.12 illustrates a face block B and its complement inside of S^3.

Taking S_B^3 to be the stratified S^3 formed as the union of B and B', we craft a stratified 2–handle structure as $C(S_B^3)$, the cone of S_B^3. We call $C(S_B^3)$ the *stratified 2–handle induced by* B. Attaching $C(S_B^3)$ to W over $B \subset M_1$ alters the boundary of W by replacing $B \subset M_1$ with B'. The full extent of this surgery can be detected by examining the edge and vertex blocks of the stratification that are incident to B.

Theorem 3.4.1. Let M be a smooth, closed, stratified, orientable 3–manifold with stratification induced by a stratifying map f, let $\mathfrak{B}$ be the set of face blocks of M_1, and let $W = M \times [0, 1]$. Consider the 4–manifold W' constructed from W as

$$W' = W \cup \{C(S_B^3)\}_{B \in \mathfrak{B}} / \sim,$$
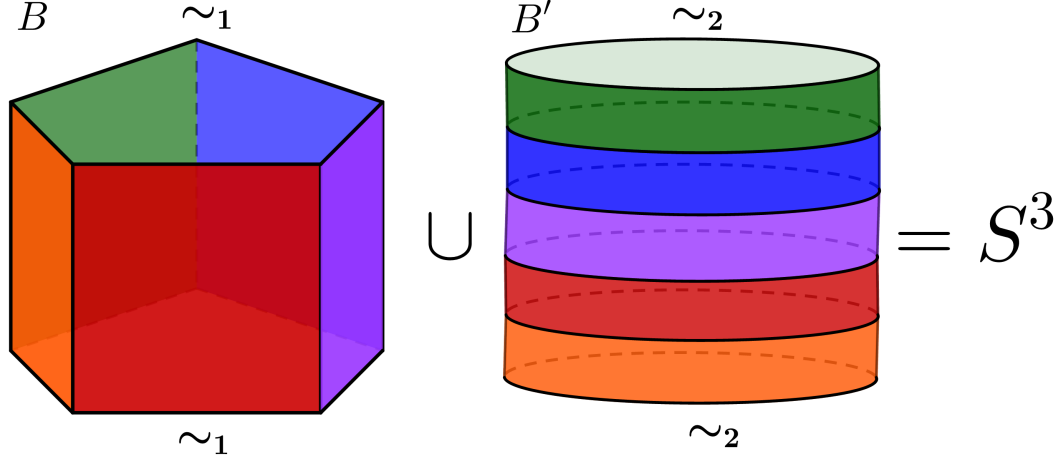
Figure 3.12: **A face block and its complement form S^3.** A face block B is a stratified closed solid torus that is stratified-homeomorphic to $S^1 \times G_n$ for some n–gon G_n. The complement of its unknotted interior in S^3 is another stratified closed solid torus B'. B and B' are depicted as cylinders with top and bottom identified.

where $\sim$ is defined by $b \sim \iota(b)$, ι the identity map $C(S_B^3) \supset B \xrightarrow{\iota} B \subset M_1$. Then $M_1' = \partial W' \setminus M_0$ is a stratified 3–manifold with a decomposition into *primed edge blocks* and *primed vertex blocks* such that the decomposition is well-defined and the primed blocks have the following structure:

> **Primed edge block:** A primed edge block E' is identical to an edge block E from Theorem 3.3.4 with (3,2)–handles (i.e. cylinders: $D^2 \times [0,1]$) attached over all annular boundary strata of E (i.e. each closed strata A of E such that $A = E \cap B$ for some face block $B \in \mathfrak{B}$). Thus E' is a stratified 3–manifold homeomorphic to $S^2 \times [0,1]$

> **Primed vertex block:** A primed vertex block V' is identical to a vertex block V from Theorem 3.3.4 with (3,2)–handles attached over each annular boundary stratum A of V such that $A = V \cap B$ for some face block $B \in \mathfrak{B}$. Furthermore, we show that V' is a stratified (3,2)–handlebody.

Proof. We split the proof of this theorem into three parts. In the first two parts, we prove that we can find the prescribed primed edge and vertex block structures in M_1'. In the third part, we show that these structures exhaust M_1'.

Part 1: Edge blocks occur in three possible forms: regular edge blocks as $A \times [0,1]$, definite edge blocks as $D^2 \times [0,1]$, and indefinite edge blocks as $P \times [0,1]$. Figure 3.13

displays the possible edge block forms and indicates the boundary strata of an edge block that are shared by face blocks.
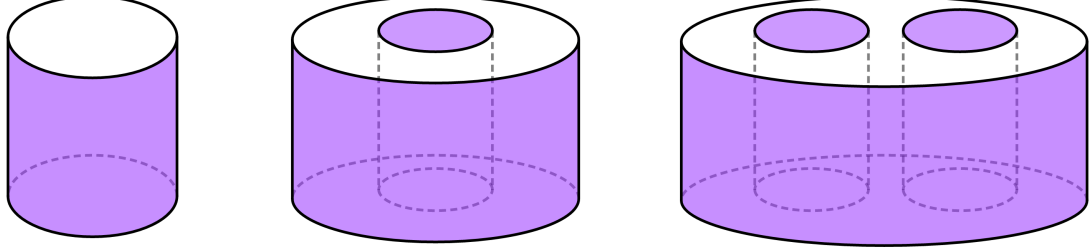
Figure 3.13: **Edge blocks.** The possible edge blocks of M_1. Annular boundary strata that are incident with face blocks of M_1 are indicated in purple. For each block, attaching (3,2)–handles over the indicated annuli results in a stratified 3–manifold homeomorphic to $S^2 \times [0,1]$.

Figure 3.14 illustrates how 2–handle attachment affects edge blocks. The effect on ∂W near E of attaching the (4,2)–handle $C(S_B^3)$ over B is equivalent to attaching a (3,2)–handle from the stratification of B' to E over the annular boundary stratum $E \cap B$. Attachment of all (4,2)–handles to W applies this (3,2)–handle attachment to all annular strata of E, and attaching these (3,2)–handles to all annular strata of E results in a 3–manifold homeomorphic to $S^2 \times [0,1]$.
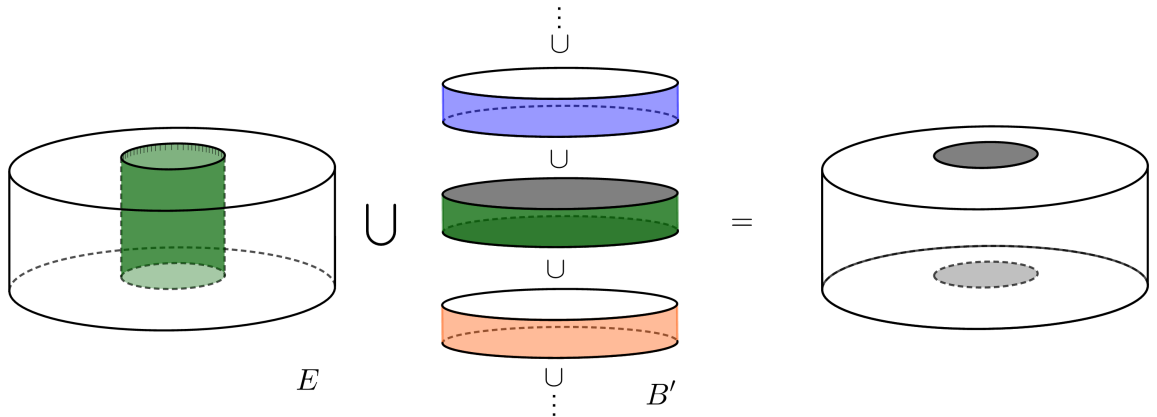
Figure 3.14: **The effect of stratified (4,2)–handle attachment on an example edge block.** An edge block E, a face block complement B', and the result of attaching $C(S_B^3)$ to W over B on E. The boundary stratum shared by E and B in M_1 is indicated in green, as is the corresponding boundary stratum of B' in S_B^3.

Part 2: Let V be a vertex block. All vertex blocks are stratified (3,1)–handlebodies of some genus, and V and V' are related via (3,2)–handle attachments to V induced

by (4,2)–handle attachments. The attaching regions are disjoint, so the resulting manifold is independent of the order in which we attach handles.

Let g be the genus of V. Proving that V' is a (3,2)–handlebody when $g = 0$ is trivial, because V is then a 3–ball. This means V' is a 3–ball with a collection of (3,2)–handles attached to it, i.e. a (3,2)–handlebody. The case of $g > 0$ is nontrivial.

Suppose V is a (3,1)–handlebody of genus $g > 0$. To prove that V' is a (3,2)–handlebody, we show that each (3,2)–handle attachment either cancels a (3,1)–handle of V or adds a new S^2 boundary component away from the (3,1)–handles of V. When $g > 0$, V is a regular neighbourhood of either a circle or one of the nontrivial singular fibers in Figure 3.5. Each case provides a (3,1)–handlebody structure for V. Because we are interested in handle cancellation, the salient point is the identification of (3,1)–handle belt spheres. When V is a solid torus, i.e. a regular vertex block, we set any meridinal circle of V as a belt sphere for the (3,1)–handle. Otherwise, give the fiber the graph structure implied by Figure 3.5. Then V has a (3,1)–handlebody structure with one or two (3,0)–handles, depending on the number of singular points in the fiber (i.e. vertices in the graph structure), and a (3,1)–handle for each edge.

With a (3,1)–handlebody structure in place, let α_i be the belt spheres of each (3,1)–handle. This implies that the α_i are pairwise non-parallel. Let β_i be the attaching spheres of the (3,2)–handles that we attach to V in the construction of V'. For each i, j, $|\alpha_i \cap \beta_j| = 0$ or 1 by construction. Moreover, every (3,1)–handle belt sphere transversely intersects at least one of the (3,2)–handle attaching spheres, every (3,2)–handle attaching sphere intersects at least one of the (3,1)–handle belt spheres. All intersection numbers are at most 1, so every (3,2)–handle attached to V either cancels out an existing (3,1)–handle or adds a new 2–sphere boundary component. Because $\partial V'$ is a disjoint collection of 2–spheres we conclude that every (3,1)–handle of V has been cancelled by a (3,2)–handle, thus V' is a (3,2)–handlebody. We present an example of how these handle attachment sites are arranged in Figure 3.15.

Part 3: To show that primed edge and vertex blocks exhaust M_1', we show that the entirety of B' has been apportioned among the primed blocks for each B'. The $(3, k)$ strata of B' are each cylinders whose annular boundary strata correspond directly to a longitudinal boundary annulus of B. Face regions do not intersect even on their boundaries, so all of the annular boundary strata of B, hence B', are shared only by edge and vertex blocks. Thus each cylinder of B' has been assigned as a (3,2)–handle and attached to a primed edge or vertex block. Because (4,2)–handle attachment altered M_1 to M_1' only by replacing each face block B with its complementary B', the
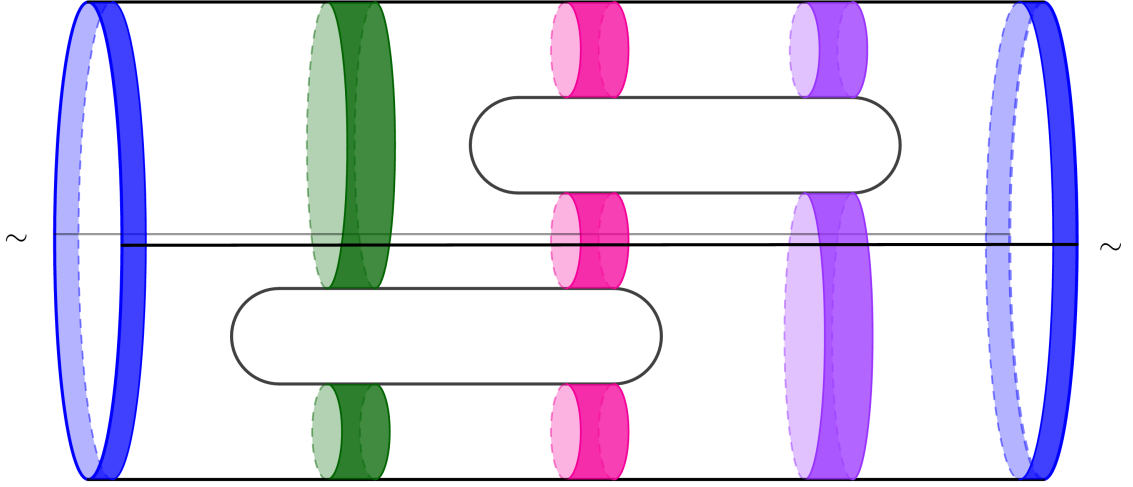
Figure 3.15: **Vertex block with (3,2)–handle attachment sites indicated.** We display an example vertex block of M_1. Recall that this is the second type of interactive vertex block and, as in Figure 3.11, the surface is presented as embedded in S^3 and the block is the stratified (3,1)–handlebody on the 'outside' of the surface in S^3. Annular boundary strata that are incident with face blocks of M_1 are indicated in color and correspond to the shared vertex-face region boundary edge. The 1–handle belt spheres are also indicated as black horizontal arcs across the surface. Attaching (3,2)–handles over the indicated annuli as prescribed results in a (3,2)–handlebody.

primed blocks must exhaust M_1'. □

3.4.2   3–handles

Decomposing M_1' into primed edge and vertex blocks provides us with stratified 3–handle attachment neighbourhoods. A 4–dimensional 3–handle is attached over an $S^2 \times [0,1]$ embedded in the boundary of a 4–manifold, so attachment neighbourhoods for our stratified 3–handles are the primed edge blocks of M_1'. We begin 3–handle attachment by precisely defining the structure of a stratified 3–handle so that it may be attached over a primed edge block.

   Let E' be a primed edge block of M_1'. By Theorem 3.4.1, E' is homeomorphic to $S^2 \times [0,1]$. In particular, $\partial E'$ is a disjoint pair of stratified 2–spheres. We form a 4–disk containing E' in its boundary by a double coning method on E': we first cone the spherical boundary components of E' to form a pair of 3–disks, glue these 3–disks to E' to form a 3–sphere, then cone the 3–sphere to obtain a 4–disk.

   For each stratified boundary sphere $S_i^2 \in \partial E'$ we form the stratified 3–disk $C(S_i^2)$

and glue $C(S_i^2)$ to E' over S_i^2. The result is a stratified 3–sphere, and we further cone that 3–sphere to form a stratified 4–disk. We denote the 4–disk by $C^2(E')$ and call the resulting stratified 3–handle structure the *stratified 3–handle induced by E'*. Attaching $C^2(E')$ to W' over $E' \subset M_1'$ alters the boundary of W' by replacing E' with the 3–disks $C(S_i^2)$ glued over the corresponding stratified boundary spheres in M_1'. The full extent of this surgery can be detected by examining the primed vertex blocks of M_1' in Corollary 3.4.2.

Corollary 3.4.2. Let W' be the 4–manifold resulting from the construction described in Theorem 3.4.1 and let $\mathfrak{E}'$ be the set of primed edge blocks of $M_1' \subset \partial W'$. Consider the 4–manifold W'' constructed from W' as

$$W'' = W' \cup \{C^2(E')\}_{E' \in \mathfrak{E}'} / \sim,$$

where $\sim$ is defined by $e \sim \iota(e)$, ι the identity map $C^2(E') \supset E' \xrightarrow{\iota} E' \subset M_1'$. Then $M_1'' = \partial W'' \setminus M_0$ is a stratified 3–manifold with a decomposition into *double primed vertex blocks V''* such that the decomposition is well-defined and each V'' is homeomorphic to S^3.

Proof. We need only prove that each connected component of M_1'' is homeomorphic to S^3. Let V' be a primed vertex block. We know that V' is a (3,2)–handlebody and $\partial V'$ is a disjoint collection of 2–spheres. Thus the attachment of (3,3)–handles to V' over each 2–sphere boundary component results in a 3–sphere, proving the theorem. $\square$

After attaching 3–handles over primed edge blocks, W'' is a 4–manifold with boundary consisting of M_0 and a collection of stratified 3–spheres. We attach stratified 4–handles over these 3–spheres, so we begin by precisely defining the structure of these handles.

3.4.3 4–handles

Let V'' be a double primed vertex block of M_1''. By Corollary 3.4.2, V'' is homeomorphic to S^3. We form a 4–disk whose boundary is V'' by taking the cone of V''. We denote this 4–disk by $C(V'')$ and call the resulting 4–handle structure the *stratified 4–handle induced by V''*. Attaching $C(V'')$ to W'' over V'' alters the boundary of W'' by replacing V'' with $\emptyset$.

Corollary 3.4.3. Let W'' be the 4–manifold resulting from the construction described in Corollary 3.4.2 and let $\mathfrak{V}''$ be the set of double primed vertex blocks of $M_1'' \subset \partial W''$. Consider the 4–manifold W''' constructed from W'' as

$$W''' = W'' \cup \{C(V'')\}_{V'' \in \mathfrak{V}''}/ \sim,$$

where $\sim$ is defined by $v \sim \iota(v)$, ι the identity map $C(V'') \supset V'' \xrightarrow{\iota} V'' \subset M_1''$. Then $M_1''' = \partial W''' \setminus M_0 = \emptyset$, hence W''' is a 4–manifold whose boundary is exactly M.

Chapter 4

Algorithm for triangulated manifolds

Algorithmic construction of a triangulated 4–manifold with prescribed closed, orientable 3–manifold boundary broadly follows the steps we used in the construction of a 4–manifold a with prescribed smooth, orientable 3–manifold boundary. Let N be a closed, orientable 3–manifold triangulation. Then the steps of construction are:

1. Define a projection $f : N \to \mathbb{R}^2$.

2. Induce a subdivision of N from f. The result is a 3–dimensional polyhedral gluing N' that is equivalent to N.

3. Subdivide N' into a 3–manifold triangulation M that is equivalent to N.

4. Form the 4–manifold triangulation $W = M \times [0, 1]$ with boundary components $M_0 = M \times \{0\}$ and $M_1 = M \times \{1\}$. This is done by gluing a 4–prism to each tetrahedron of M.

5. Attach 4–dimensional 2–handles to W over its M_1 boundary as prescribed by the subdivision of M from f. Call the result W' and let $M_1' = \partial W' \setminus M_0$.

6. Form W'' by attaching 4–dimensional 3–handles to W' over M_1' as prescribed by the subdivision induced by f and the surgery induced by 2–handle attachment.

7. The boundary of W'' consists of M_0 and a collection of copies of S^3. Attaching a 4–handle to each S^3 boundary component results in a triangulated 4–manifold whose boundary is exactly M_0.

This construction has input a closed, orientable 3–manifold triangulation N and output a 4–manifold triangulation W''' whose sole boundary component is a triangulated 3–manifold that is equivalent to N. In this case, we find that $\partial W'''$ is a subdivision of N, and this subdivision is the subdivision induced by the projection f in Step 1.

It is necessary that the input 3–manifold triangulation is *edge-distinct*, i.e. if u, v are vertices of N then $\{u, v\}$ is the boundary of at most one edge. If this condition is not satisfied by a given N, then it is satisfied by the barycentric subdivision of N. We assume that N is edge-distinct for the remainder of the chapter.

Throughout this chapter N refers to the input closed, orientable 3–manifold triangulation, f refers to the subdividing map defined in Section 4.1, M is the subdivision of N induced by f, W is the 4–manifold triangulation obtained from $M \times [0, 1]$, W' is the result of attaching 2–handles to W, and W'' is the result of attaching 3–handles to W'.

4.1   Define projection

In this algorithm, we use a projection of $f : N \to \mathbb{R}^2$ in the same way that we used a stratifying map in Chapter 3: preimages of sleeves around important features of the projection in the plane define handle attachment sites. The important features are the images of the 1–skeleton of N, and we want a high amount of control over how we construct these features in the plane. We first lay out conditions required of the projection, describe a method for ensuring these conditions are met, and then turn the method into an algorithm. We do all of this before forming the base 4–manifold so that the boundary components of W contain the desired handle attachment sites.

Our subdivision of N is obtained by imposing four conditions on $f : N \to \mathbb{R}^2$:

1. f maps vertices to the circle, i.e. for each vertex $v \in N^0$, $f(v)$ lies on the unit circle in $\mathbb{R}^2$.

2. The images of vertices are distinct, i.e. for every pair of vertices $u, v \in N^0$, $f(u) \neq f(v)$.

3. f is linear on each simplex of N and piecewise-linear on N, i.e. if $x \in \sigma$ is a point in the simplex σ with vertices v_i, then $x = \sum_i a_i v_i$ with $\sum_i a_i = 1$ and $f(x) = \sum_i a_i f(v_i)$.

4. Edge intersections are distinct, i.e. for every triple of edges $e_1, e_2, e_3 \in N^1$ that share no vertices, $f(e_1) \cap f(e_2) \neq f(e_2) \cap f(e_3)$.

We call these the *subdivision conditions* on f, and we call a map satisfying the subdivision conditions a *subdividing map*. Conditions 1 and 2 ensure that every simplex of N is mapped to the plane in standard position, where a simplex σ of N is mapped to the plane in *standard position* if every point in $f(\sigma^0)$ is essential in forming the convex hull of $f(\sigma^0)$ as shown in Figure 4.1. This, along with conditions 3 and 4, allows us to use concepts and language from normal surface theory to describe the subdivision of N in the next section.

All conditions are satisfied by fixing an odd integer k greater than or equal to the number of vertices in N, injecting the vertices of N to the kth complex roots of unity in the plane, then extending linearly over the skeletons of N. The first three conditions are clearly satisfied by this procedure, and the last is satisfied by the results in [9].

Algorithm 1 takes as input the closed, orientable 3–manifold triangulation N and produces a subdividing map $f : N \to \mathbb{R}^2$. The subdividing map projects each tetrahedron to the plane in *standard position*, as shown in Figure 4.1.

Data: A closed, orientable 3–manifold triangulation N
Result: A subdividing map $f : N \to \mathbb{R}^2$
1 **begin**
2    $k =$ the smallest odd number greater than or equal to $|N^0|$
3   **foreach** *vertex v_i in N^0, $i = 1, \ldots, |N^0|$* **do**
4      $f(v_i) = (\cos(\frac{2\pi i}{k}), \sin(\frac{2\pi i}{k}))$
5   **end**
6   **foreach** *n in $\{1, 2, 3\}$* **do**
7   **foreach** *simplex σ in N^n* **do**
8   By definition, σ is the set of convex combinations of σ^0:
9          $\sigma = \{x \mid x = \sum_{i=0}^{n} a_i v_i, \sum a_i = 1, a_i \geq 0, v_i \in \sigma^0\}$
10   Define f on $x \in \sigma$ by requiring linearity over simplices:
11          $f(x) = f(\sum_{i=0}^{n} a_i v_i) = \sum_{i=0}^{n} a_i f(v_i)$
12   **end**
13   **end**
14 **end**

Algorithm 1: Constructing a subdividing map for a 3–manifold triangulation
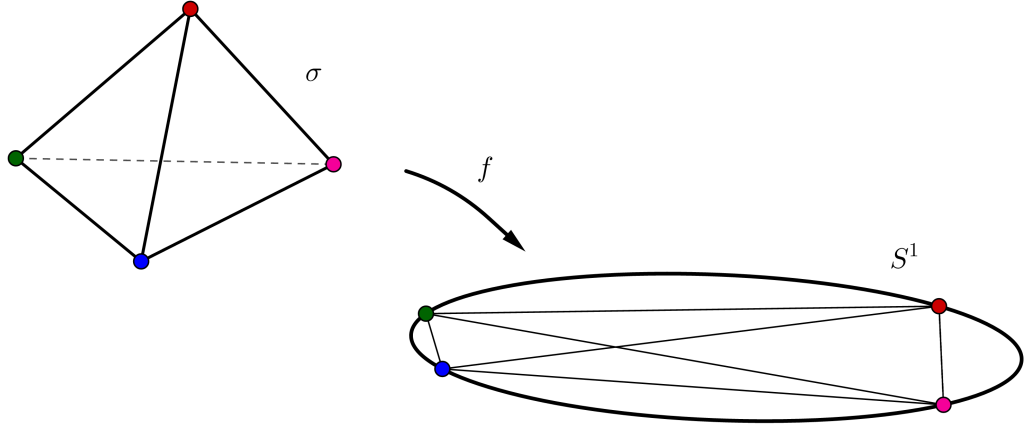
Figure 4.1: **A tetrahedron σ projected to the plane in standard position through a subdividing map f.** The four vertices of σ^0 map to the unit circle in the plane, thus form a convex arrangement. Four of the six edges of σ^1 map to the boundary of $f(\sigma)$, connecting $f(\sigma^0)$. The last two edges map across $f(\sigma)$, forming an intersection interior to $f(\sigma)$. Each vertex of the arrangement is essential in forming the convex hull of $f(\sigma^0)$.

4.2 Induce subdivision

The goal of subdividing N is to create and identify handle attachment sites analogous to the face, edge, and vertex blocks of Chapter 3. We use a similar technique to that found in Chapter 3, iteratively subdividing the tetrahedra of N by certain preimages of f. Tetrahedron subdivisions are compatible, i.e. tetrahedron subdivisions fit together exactly as the undivided tetrahedra do inside of N.

We perform two subdivisions and one 4–thickening in this chapter. The first is from the triangulation N into the polyhedral gluing N', and this produces combinatorial blocks. The second is the subdivision of N' into an equivalent triangulation M, preserving the combinatorial blocks. The 4–thickening is completed by attaching 4–prisms to every tetrahedron of M, gluing the prisms over their walls.

4.2.1 Triangulation to Polyhedral Gluing

Let σ be a tetrahedron of N and let s be a line segment in the plane such that $s \cap f(\sigma)$ is nonempty, the endpoints of s are outside of $f(\sigma)$, and $s \cap f(\sigma)$ is a line segment in $f(\sigma)$ disjoint from any vertices or crossings of $f(\sigma)$. Figure 4.2 demonstrates the possible configurations of these line segments, and shows that their preimages inside of σ are triangles and quadrilaterals (or *quads*). We refer to these preimages as

exterior triangles and *exterior quads*. When a pair of these preimages intersect, the intersection is a line segment with endpoints interior to a pair of triangles of σ^2.
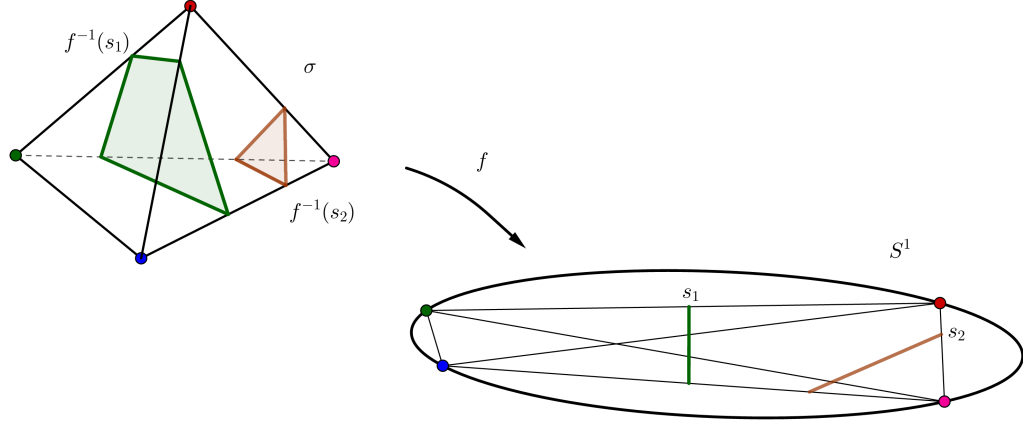
Figure 4.2: **A tetrahedron σ in standard position, intersecting edges, and preimage triangles and quads.** An intersecting edge separates the vertices of σ. If one is separated from the other three, its preimage is a triangle. If the vertices are separated into two pairs of two, the preimage is a quad.

For each $\sigma \in N^3$ and each edge e of N^1 such that $e \notin \sigma^1$, $f(e)$ is a line segment in the plane that is either disjoint from $f(\sigma)$ or induces an exterior triangle or quad in σ. The image of σ is a quadrilateral in the plane, and four of σ's edges map to the boundary of that quadrilateral. The remaining two edges are the *interior edges* of σ, and the subdividing preimage triangles they induce in σ are *interior triangles*. Figure 4.3 shows one interior triangle along with its possible intersections with exterior triangles and quads. The interior triangles of σ always intersect in a line segment with endpoints inside of the interior edges of σ, shown in Figure 4.4

Recall that the goal of this subdivision is to identify combinatorial analogues for the face, edge, and vertex blocks of Chapter 3. If we were to subdivide N using the quads and triangles induced by the edges of N, such blocks are ill-defined. We amend this by introducing a set of line segments analogous to the sleeves of Section 3.2.

The vertices of N are sent to the edge of the boundary of the disc in the plane, and this boundary is the only location in the plane where our smooth singularity theory does not apply. Our first set of line segments remedies this. Let p be a vertex of N and s a secant in the disc that separates $f(p)$ from $f(N^0 \setminus p)$. Then $f^{-1}(s)$ is a triangulated 2–sphere, and is the boundary of a triangulated 3–disc centred at p. We use such 3–discs as our first collection of combinatorial vertex blocks
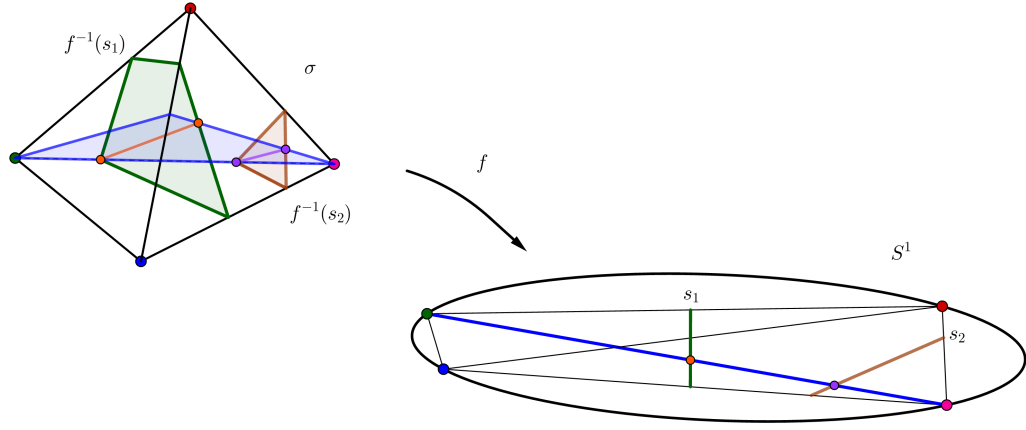
Figure 4.3: **A tetrahedron σ in standard position, one interior triangle, one exterior triangle, and one exterior quad.** There are two special preimage triangles in σ, called *interior triangles*, that occur as the preimages of the edges of σ that map through f across $f(\sigma)$ as in Figure 4.1.
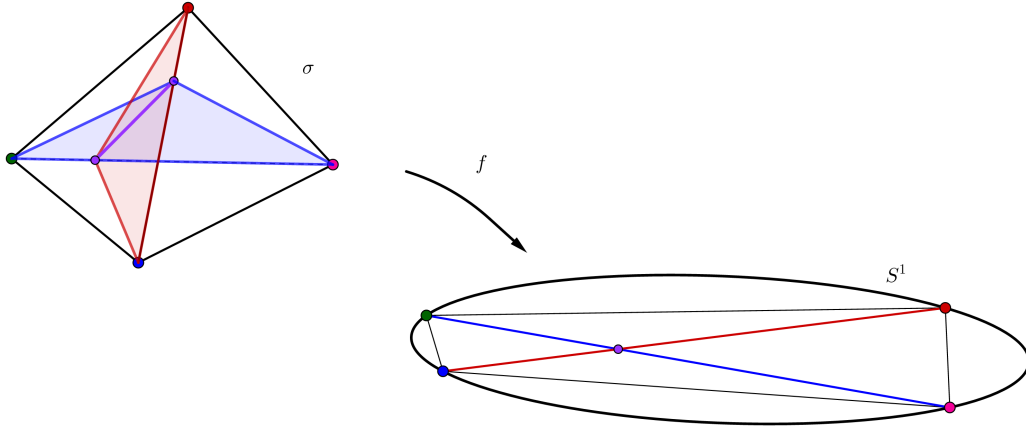
Figure 4.4: **A tetrahedron σ in standard position with both interior triangles.** As in Figure 4.3, but displaying both interior triangles.

The vertices of N are mapped to the kth roots of unity and the rest of the simplices of N are mapped to the plane via linear extension. Consider the regular k–gon G_k with vertices the kth roots of unity reflected through the origin. Because k is odd, each of G_k's edges is a secant in the disc that separates the image of one vertex of N from the rest. Moreover, G_k separates $f(N^0)$ from the interior edge-edge crossings of $f(N)$. We use G_k as our first set of line segments.

Next, we introduce segments that induce the edge and face blocks and the rest of the vertex blocks. For each edge e of N^1, consider $e_\varepsilon^+ = s(e + \varepsilon_e e_\perp)$ and $e_\varepsilon^- = s(e - \varepsilon_e e_\perp)$, secants in G_k that are parallel to $f(e)$ and located a small orthogonal

distance away from $f(e)$. Here we are using $s(\cdot)$ as a function that extends and trims line segments in the plane into secants in G_k. We require that our ε's are small enough that if $e, g \in N^1$ share a boundary vertex then $e_\varepsilon^\pm$ and $g_\varepsilon^\pm$ do not intersect (i.e. G_k truncates the segments so that their intersection occurs outside of G_k). The segments $e_\varepsilon^\pm$ for each $e \in N^1$ are called *sleeve segments*, and their preimages form exterior triangles and quads inside of the tetrahedra of N. Figure 4.5 depicts the inclusion of G_k and all sleeve segments for a mapping of a triangulated S^3 to the plane. Here, the triangulation of S^3 used is the 2-tetrahedron triangulation.
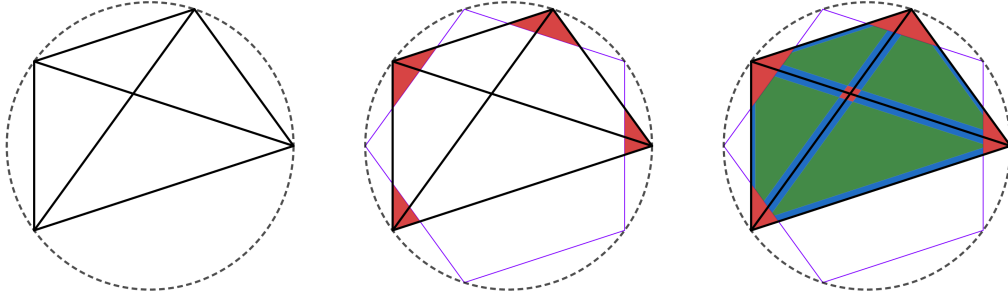
Figure 4.5: **The process of including additional segments into the plane to form piecewise-linear sleeves.** From left to right, we see first the image of the 1–skeleton of N mapped to the plane, then the inclusion of the regular polygon G_5, which forms (red) vertex sleeves around the image of each vertex of N. The rightmost image depicts all sleeve segments as secants of G_5, forming the remaining (red) vertex sleeve, six (blue) edge sleeves, and four (green) face sleeves that subdivide N.

Take L to be the set of line segments in the plane. This consists of each segment of G_k, $f(e)$ for each $e \in N^1$, and the sleeve segments $e_\varepsilon^\pm$. For each tetrahedron σ of N, the polygons and intersections of $f^{-1}L \cap \sigma$ define a subdivision of σ into a cell complex. We implement this subdivision in Algorithm 2 by constructing a new cell complex that is equivalent to N. The subdivision iterates over all of the triangles and quads inside of σ, and the subdivision induced by a polygon is fully realized before moving on to the next.

For an example of subdivision, refer to Figure 4.3, where a tetrahedron is being subdivided by an exterior triangle, an interior triangle, and an exterior quad. We construct the subdivision of σ as a 3–complex τ, starting by setting $\tau = \sigma$. Starting at the loop on line 6 of Algorithm 2, p. 41, we'll assume that the brown segment that separates the pink vertex from the rest of $f(\sigma)$ is a segment from G_k and set this segment as l. This makes δ on line 7 the brown exterior triangle in σ. Then the loop on line 8 runs over all 1–cells of τ that intersect the exterior triangle δ which are the

three 1–cells of τ incident with the pink vertex. We subdivide these 1–cells by their intersection with δ, which amounts to including the corners of the δ exterior triangle into the complex, splitting the relevant 1–cells into a pair of 1–cells on either side of the corner. This subdivision turns the three boundary triangles of τ that contained the pink vertex into pentagons. We move to the loop on line 12, where we subdivide these three boundary pentagons by the three triangular edges of δ. Each pentagon is subdivided into a triangle and a quadrilateral. Finally, in the loop at line 16 we subdivide the only 3–cell of τ into a tetrahedron containing the pink vertex and a triangular cylinder away from the pink vertex.

Heading back to the top of the loop at line 6 and assuming we have exhausted all segments of G_k, we may now consider any segment. Setting l to be the blue interior edge of Figure 4.3 makes δ the blue interior triangle. Moving through the loop at line 8, we find

1. the intersection of δ with the 1–cell of τ containing the blue and red vertices and

2. the intersection of δ with the brown exterior triangle located on the shared boundary of the pair of 2–cells in $\partial\tau$ induced by the subdivision of the 2–cell in $\partial\sigma$ opposite the green vertex.

We then insert 0–cells into τ at these intersections, subdividing 1–cells as necessary. The loop at line 12 now runs over the intersections of δ with the 2–cells of τ, and these intersections occur with the triangle in $\partial\tau$ opposite the pink vertex and with the 2–cells in $\partial\tau$ induced by the subdivision of the 2–cell in $\partial\sigma$ opposite the green vertex. We add 1–cells to τ that divide the quadrilateral into a pair of quadrilaterals and the triangles into pairs of triangles. Finally, the loop at line 16 subdivides both 3–cells of τ, splitting them each in half as polyhedrons. It is left to the reader to continue the subdivision of τ in Figure 4.3, where the remaining exterior quad subdivides five 1–cells, five 2–cells, and two 3–cells.

Observe also that the gluing defined on the tetrahedra of N is used to produce N' as well. To see this, let σ and σ' be tetrahedra of N that are glued together over a triangular face, $\Delta \in \sigma$ and $\Delta' \in \sigma'$. Then Algorithm 2 produces a pair of 3–complexes τ and τ', and Δ, Δ' are each subdivided into boundary 2-complexes of τ and τ'. These subdivisions are induced by the subdivisions of $f(\Delta)$ and $f(\Delta')$ in the plane but, because Δ and Δ' are identified in the gluing of N, $f(\Delta) = f(\Delta')$ and

the subdivisions of Δ and Δ' are equivalent. The gluing that defines N' is therefore constructed by subdividing the gluing that defined N.

Data: A closed, orientable 3–manifold triangulation N with subdividing map $f : N \to \mathbb{R}^2$

Result: A closed, orientable 3–dimensional polyhedral gluing N' that is a subdivision of N

1 **begin**
2 $\quad$ $L = G_k \cup \{f(e) \mid e \in N^1\} \cup \{e_\varepsilon^\pm \mid e \in N^1\}$
3 $\quad$ **foreach** *tetrahedron σ of N^3* **do**
4 $\quad\quad$ We construct a 3–dimensional cell complex τ that is the subdivision of σ prescribed by f
5 $\quad\quad$ $\tau = \sigma$
6 $\quad\quad$ **foreach** *segment l in L such that $l \cap f(\sigma) \neq \emptyset$ and $l \nsubseteq \partial f(\sigma)$, iterating over the segments of G_k first* **do**
7 $\quad\quad\quad$ $\delta =$ the intersection of σ with $f^{-1}l$
8 $\quad\quad\quad$ **foreach** *intersection $d_0 \in \delta \cap \tau^1$ such that $d_0 \notin \tau^1$* **do**
9 $\quad\quad\quad\quad$ $d_0 = \delta \cap t_1$ for some 1–cell t_1 of τ
10 $\quad\quad\quad\quad$ Subdivide t_1 by d_0 into a pair of 1–cells td_1 and dt_1
11 $\quad\quad\quad$ **end**
12 $\quad\quad\quad$ **foreach** *intersection $d_1 \in \delta \cap \tau^2$* **do**
13 $\quad\quad\quad\quad$ $d_1 = \delta \cap t_2$ for some 2–cell t_2 of τ
14 $\quad\quad\quad\quad$ Subdivide t_2 by d_1 into a pair of 2–cells td_2 and dt_2
15 $\quad\quad\quad$ **end**
16 $\quad\quad\quad$ **foreach** *intersection $d_2 \in \delta \cap \tau^3$* **do**
17 $\quad\quad\quad\quad$ $d_2 = \delta \cap t_3$ for some 3–cell t_3 of τ
18 $\quad\quad\quad\quad$ Subdivide t_3 by d_2 into a pair of 3–cells td_3 and dt_3
19 $\quad\quad\quad$ **end**
20 $\quad\quad$ **end**
21 $\quad$ **end**
22 $\quad$ $N' =$ the set of 3–complexes τ constructed above, glued together as prescribed by the gluing maps of N and the identification of the τ as subdivisions of the tetrahedra of N
23 **end**

Algorithm 2: Using a subdividing map to subdivide the input 3–manifold triangulation

---

We subdivided N into N' in order to identify analogues to the face, edge, and vertex blocks of Chapter 3. The analogous blocks are defined exactly as they were in Chapter 3 — the sleeve segments subdivide the plane into regions homeomorphic to disks, those disks are classified by whether they contain a crossing of $f(N^1)$, intersect

$f(N^1)$ but do not contain a crossing, or do not intersect $f(N^1)$ at all. The preimage of a region that contains a crossing is a *combinatorial vertex block*, the preimage of a region that intersects $f(N^1)$ but does not contain a crossing is a *combinatorial edge block*, and the preimage of a region that is disjoint from $f(N^1)$ is a *combinatorial face block*. Symmetric names are used for the regions that these blocks project onto — combinatorial face (resp. edge, vertex) blocks map through f to *combinatorial face (resp. edge, vertex) regions.* Figure 4.5 illustrates the regions in the plane that produce such blocks. These preimages exhaust the cells of N', providing a decomposition into subcomplexes. This decomposition is not a partition — some cells are assigned to more than one block. Such an assignment happens precisely when a cell is mapped through f to the shared boundary of different combinatorial regions.

4.2.2 Polyhedral Gluing to Triangulation

Algorithm 2 produces a cell complex N' that is a polyhedral gluing, and we would prefer to replace N' with an equivalent triangulation. This is done by first replacing each polyhedron P that is not a tetrahedron with the cone on ∂P. At each polyhedron P this replaces the single 3–cell interior of P with $|P^2|$ new polyhedra, each of which has at most one non-triangular face. Because N' is closed, that face is glued to another face of the same polygonal type. If P, Q are a pair of polyhedra of N' that are glued over the faces P_i^2 and Q_j^2, each of which is a k–gon, $k > 3$, then we further subdivide $P_i^2 \sim Q_j^2$ into $k - 2$ triangles, and replace the newly introduced polyhedra with $k - 2$ new tetrahedra, as illustrated in Figure 4.6. This process thus adds $2k - 4$ tetrahedra per k–gon 2–cell of N', $k > 3$. Note that if the boundary of P and Q is not essential in the decomposition of N' into blocks, i.e. is not contained in the boundary of some combinatorial block, then we can instead replace the polyhedra incident to that face with the more efficient (when $k > 4$) triangulation of the suspension of the k–gon with k tetrahedra, also illustrated in Figure 4.6. The further subdivision of N' into the equivalent triangulation M is detailed in Algorithm 3.

4.2.3 Thickening a Triangulation

Next, we form the 4–thickening $W = M \times [0, 1]$. This is done by attaching triangulated 4–prisms to each tetrahedron of M, where a triangulated 4–prism is the 4–dimensional extension of the triangulated 3–prism described in Theorem 3.1 of [2]. Specifically,

Data: A closed, orientable 3–manifold N' expressed as a 3–dimensional polyhedral gluing

Result: A closed, orientable 3–manifold triangulation M that is a subdivision of N'

1 **begin**
2   $M = N'$
3   **foreach** *polyhedral 3–cell τ of M that is not a tetrahedron* **do**
4   Replace τ with the cone on $\partial\tau$
5   **end**
6   **foreach** *polygonal 2–cell δ of M that is not a triangle* **do**
7   δ is the shared boundary of the polyhedral 3–cells τ_+ and τ_-
8   Each of τ_+, τ_- contains one vertex that is disjoint from δ
9   Call these vertices v_+, v_- respectively
10   Delete τ_+ and τ_- from M
11   Subdivide δ using $|\delta^0| - 2$ triangles
12   **foreach** *new 1–cell e in the triangulation of δ* **do**
13   Attach triangles over e and v_+ and over e and v_-
14   **end**
15   **foreach** *triangle f in the triangulation of δ* **do**
16   Attach tetrahedra over f and v_+ and over f and v_-
17   **end**
18   **end**
19 **end**

Algorithm 3: Triangulating a polyhedral gluing

the $(n+1)$-prism triangulation is constructed as the cone of the triangulated n–sphere whose 'top' and 'bottom' are n–simplices and whose 'sides' are the triangulated n–prism, where the triangulated 1–prism is a single edge connecting a pair of vertices. Triangulated 1–, 2–, and 3–prisms are illustrated in Figure 4.7. We use prisms at this stage because the 'walls' of the prisms are identical, making the gluing of prisms automatic. Denoting the number of n–simplices used to triangulate the n–prism by $p(n)$, and setting $p(1) = 1$, we find that

$$p(n) = 2 + n \cdot p(n-1)$$

due to the recursive nature of prism construction. This means a 2–prism is triangulated with 4 triangles, a 3–prism with 14 tetrahedra, and a 4–prism with 58 pentachora. Algorithm 4 details the 4–thickening of a closed 3–manifold.
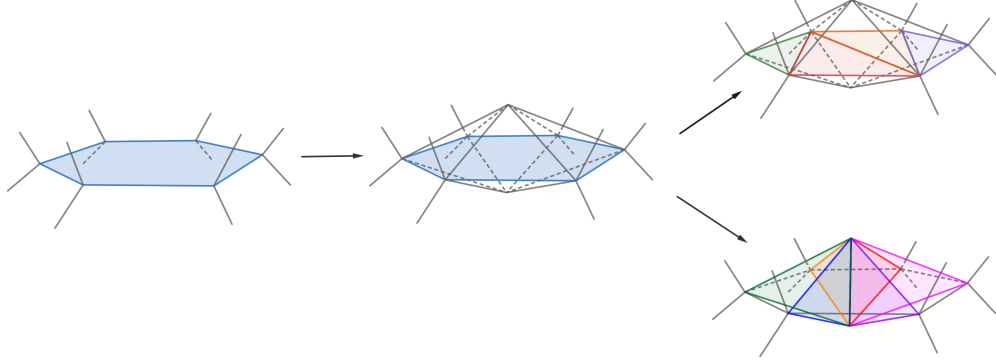
Figure 4.6: **Subdividing polyhedral cells.** From left to right, we see first the polygonal boundary 2–cell between a pair of polyhedral cells. Next, the polyhedral cells are subdivided by replacing them with the cone of their boundaries. Finally, either the polyhedra on each side of the polygon are subdivided into reflection-identical triangulations or the pair is replaced by a k simplex triangulation of the suspended k–gon.

$n = 1$ $\qquad\qquad\qquad$ $n = 2$ $\qquad\qquad\qquad$ $n = 3$
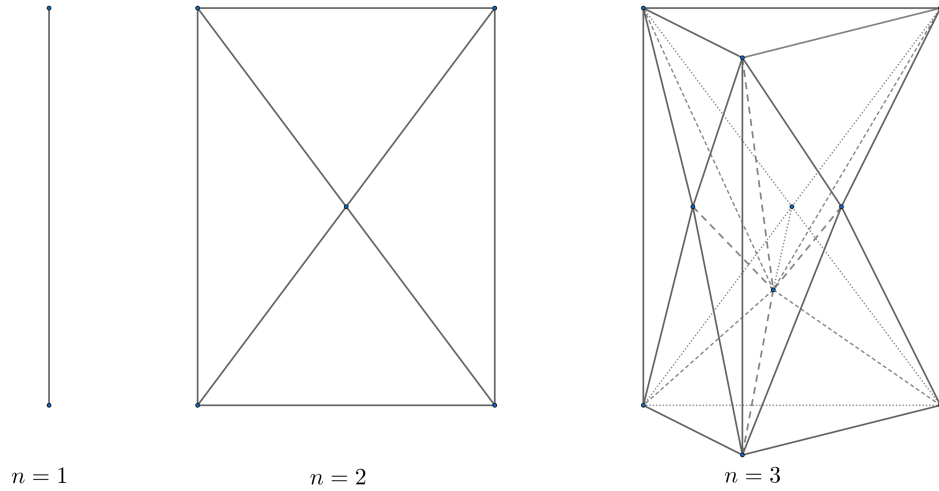
Figure 4.7: **The first three triangulated prisms.** From left to right, we see the triangulated prisms with identical walls in dimensions 1, 2, and 3.

4.2.4 Extending Smooth Singularity Theory

Before building and attaching handles, we must ensure that our smooth singularity theory adapts to the piecewise linear case. We do this by examining our combinatorial blocks. As in the smooth case, a combinatorial face block is a triangulated solid torus, a combinatorial edge block has the structure of an interval crossed with a triangulated surface that projects over a small transversal to the corresponding edge sleeve, and

```
    Data: A closed, orientable 3–manifold triangulation M
    Result: A 4–manifold triangulation W that is exactly M × I
  1 begin
  2 │   W = {P_τ | τ ∈ M³}, where each P_τ is a 4–prism with identical walls
  3 │   foreach triangle δ ∈ M² do
  4 │   │   δ is the shared boundary of the tetrahedra σ and τ
  5 │   │   Attach the prisms P_σ and P_τ of W to one another over the walls of
  6 │   │     each that correspond to δ
  6 │   end
  7 end
```

Algorithm 4: 4-thickening a closed 3-manifold

a combinatorial vertex block has the structure of a regular neighbourhood of the 1–dimensional subcomplex over its planar vertex. For combinatorial vertex blocks, this amounts to being a (3,1)–handlebody and this handlebody is determined by how its boundary surface is constructed. However, this boundary surface is the union of subtriangulations of combinatorial edge block boundaries, and these subtriangulations are precisely the surfaces that project over small transversals to the edge sleeve, making these surfaces perhaps the most topologically interesting structure in our construction. For our construction to be correct when we attach 2–handles, these surfaces must all be of genus zero, i.e. must be multiply punctured 2–spheres. This is because 2–handle attachments need to transform combinatorial edge blocks into copies of $S^2 \times D^1$. We first inspect some worked examples that have genus zero, then provide a general proof.

Each edge e of N is mapped to a secant of the circle, splitting the disc into exactly 2 sectors: the 'left' and 'right' sides of $f(e)$. Denote the set of tetrahedra of N containing e by $\Delta(e)$. Each tetrahedron σ of $\Delta(e)$ is either mapped to the left of e, to the right of e, or across e based on the image of the edge in σ opposite e.

First, we consider the situation when all of the tetrahedra containing e are mapped to the same side of $f(e)$. This happens, for example, when $f(e)$ is on the boundary of $f(N)$ and in this situation e is analogous to a definite fold. Let γ be the boundary between an edge sleeve around a section of e and an adjacent vertex sleeve. Then γ is a short interval transverse to e and we show that the preimage of γ in $\Delta(e)$ is a triangulated 2–disc.

The interval is triangulated with two edges and three vertices: one vertex at each of the sleeve segments around $f(e)$ and one vertex on $f(e)$. We'll call these vertices
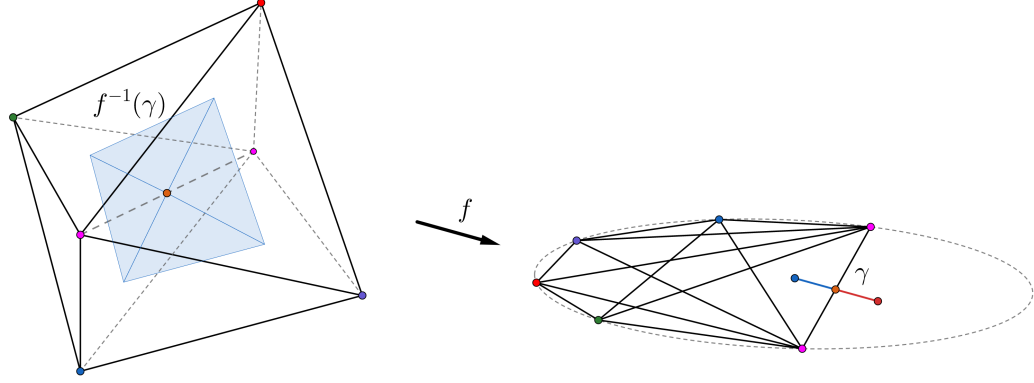
Figure 4.8: **An edge link and its image through a subdividing map.** We see the 2–disc triangulation, where the preimage of the boundary point of γ in the image of f is a single triangulated circle and that circle is wholly contained in the tetrahedra incident to the edge γ transverses.

x, y, z, letting x be the vertex on the side of e that $\Delta(e)$ is mapped to and y the vertex on $f(e)$. In M, our subdivision of N, $f^{-1}(x) \cap \Delta(e)$ is a triangulated circle, $f^{-1}(y) \cap \Delta(e)$ is a single vertex, and $f^{-1}(z) \cap \Delta(e)$ is empty. The preimage of the edge $[x, y]$ in γ forms the triangles that complete the 2–disc we expected to find, illustrated in Figure 4.8.
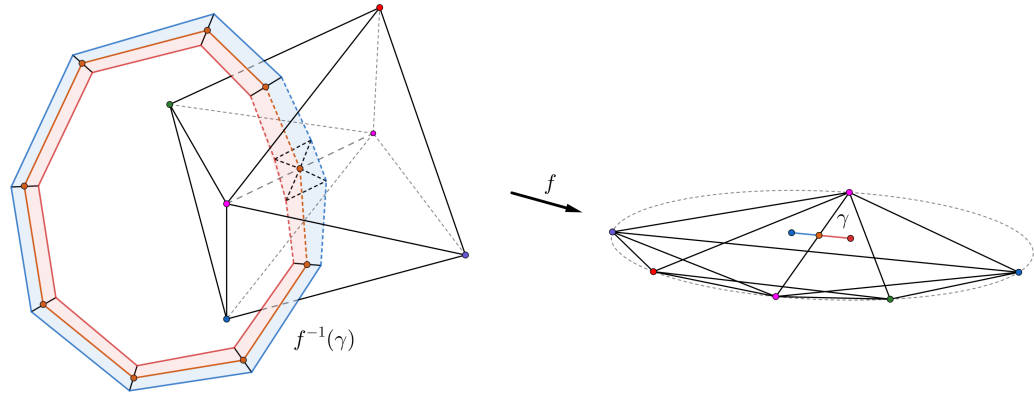
Figure 4.9: **A transversal surface around an edge e when exactly one pair of tetrahedra map across $f(e)$.** The transversal γ has two halves, one on either side of $f(e)$. Lifted to N, $f^{-1}(\gamma) \cap \Delta(e)$ is a disc incident to $\partial\Delta(e)$ in exactly two (2,1)–handle attachment sites, and the (2,1)–handle attachment is orientation preserving.

What happens when a tetrahedron of $\Delta(e)$ is mapped across $f(e)$? Because N is closed, the number of tetrahedron in $\Delta(e)$ that map across $f(e)$ is always even. The tetrahedra of $\Delta(e)$ have a circular order defined by edges in $\Delta(e)$ that are opposite e, and all tetrahedra between a crossing pair are mapped to the same side of $f(e)$.

When the number of crossing pairs is exactly one, we have a situation analogous to that of the regular edge block. The tetrahedra of $\Delta(e)$ that map to one side of $f(e)$ each contribute a single triangle to the surface $f^{-1}(\gamma)$, and the tetrahedra that map across $f(e)$ cause the disc that is $f^{-1}(\gamma) \cap \Delta(e)$ to lie incident to the boundary of $\Delta(e)$, as depicted in Figure 4.9. This boundary portion of $f^{-1}(\gamma) \cap \Delta(e)$ is a pair of $(2,1)$–handle attachment sites, but because there are only two sides of $f(e)$ in the disc the handle is attached in an orientation preserving way.
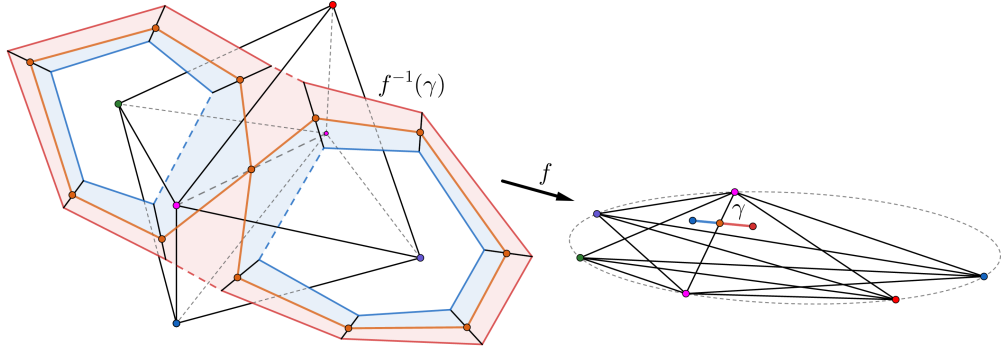
Figure 4.10: **A transversal surface around an edge e when exactly two pairs of tetrahedra map across $f(e)$.** When two pairs of tetrahedra map across $f(e)$ we find two pairs of $(2,1)$–handle attachment sites and the handle attachment is still orientation preserving. The pairing of attachment sites is determined by the structure of N: the $(2,1)$–handle attachments could be different in N, with the sites near the red and blue vertices being connected rather than the green and purple sites as depicted in the figure. However, the identification of sites across the disc $f^{-1}(\gamma) \cap \Delta(e)$ is not possible because such a handle attachment would not be orientation preserving.

When multiple tetrahedra of $\Delta(e)$ map across $f(e)$, the idea generalizes. If $2n$ such tetrahedra map across $f(e)$, then there are $2n$ $(2,1)$–handle attachment sites in $f^{-1}(\gamma) \cap \partial\Delta(e)$, these handles are attached in an orientation preserving way, and the pairing of attachment sites depends on the topology of N outside of $\Delta(e)$. Figure 4.10 shows a possible resolution of the case $2n = 4$, where we always obtain a pair-of-pants surface (note that the only handle attachments that would not produce a pants surface are not orientation preserving). Moreover, every surface in the disjoint collection of surfaces $f^{-1}(\gamma)$ is a (multiply) punctured 2–sphere. The surface of $f^{-1}(\gamma)$ that intersects $\Delta(e)$ is an $(n+1)$–punctured 2–sphere, and all other surfaces are twice-punctured (i.e. annuli).

Lemma 4.2.1. Let N be a closed, orientable 3–manifold triangulation and let M be a 3–manifold triangulation formed by applying Algorithms 1–3 to N. Let γ be the

boundary between a combinatorial edge sleeve and a combinatorial vertex sleeve, and let $f^{-1}\gamma$ be the transversal surface above γ. Then $f^{-1}\gamma$ has genus zero.

Proof. We first examine the exterior vertex sleeves — the vertex sleeves located on the boundary of the disc that M is projected onto. If v is a vertex of N, then the vertex block around v is a triangulated 3–disc, hence has 2–sphere boundary. As depicted in Figure 4.11, this 2–sphere boundary maps through f over the boundaries of face and edge sleeves. The boundaries of face sleeves lie under annuli, the boundaries of edge sleeves lie under transversal surfaces, and the S^2 boundary of the vertex block around v in M is the union of all such surfaces over their boundary circles. Genus is additive under this union, so all of the singular transverse surfaces must have genus zero.
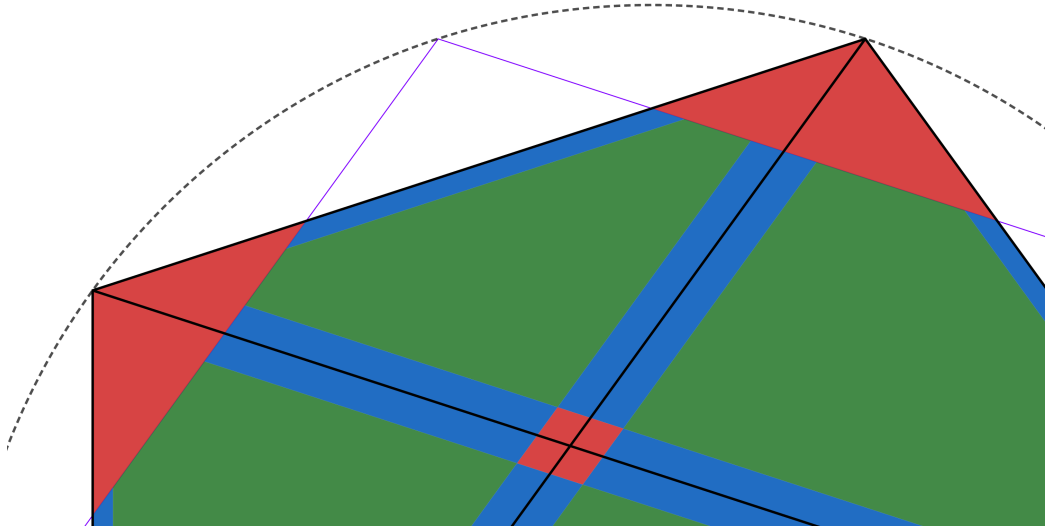
Figure 4.11: **A magnification of vertex and edge sleeve boundaries from Figure 4.5.** A boundary combinatorial vertex sleeve intersects combinatorial face and edge sleeves at intervals, while an internal vertex sleeve intersects face sleeves at points and edge sleeves at intervals.

Moving to internal transversal surfaces, let H be a vertex block, $f(H)$ the internal sleeve below H, and e, e' the pair of edges of N whose crossing induced the vertex sleeve. Then $f(H)$ has boundary constructed from transversals over e, e', two from each edge on opposite sides of $f(H)$, and we'll call these transversals γ_i, $i = 1 : 4$. Then $f^{-1}(\gamma_i)$ is a disjoint collection of triangulated surfaces in M for each i, and we'll

denote the surface incident with H by

$$\Sigma_i = H \cap f^{-1}(\gamma_i).$$

Then the boundary of H is given by

$$\partial H = \bigcup_{i=1}^{4} \Sigma_i.$$

Now suppose Σ_i has genus at least 1 for some i. This means there is a pair of curves J, K in Σ_i that are essential in the surface formed by filling in the boundary components of Σ_i with discs, the oriented intersection number of J and K is exactly 1, and $J \cup K$ is disjoint from the surfaces Σ_j for $j \neq i$. The vertex block H is a triangulated (3,1)–handlebody, so one of J, K is meridinal in H, say J.

The block H is a (3,1)–handlebody because H is a regular neighbourhood of the triangulated wedge of circles above $f(e_1) \cap f(e_2)$ in M, so all meridinal discs of H are mapped bijectively to the vertex sleeve $f(H)$. Specifically, meridians of H are mapped bijectively to $\partial f(H) = \cup_i \gamma_i$, but J is a meridian and $f(J) \subseteq \gamma_i$ for a single γ_i. This contradicts the supposition that some Σ_i has positive genus, hence the genus of Σ_i is 0 for each i. $\qquad \square$

4.3 Attach Handles

At this point in the chapter we have constructed a 4–manifold triangulation W with two boundary components, each equivalent via subdivision to the 3–dimensional cell complex M obtained in Section 4.2. Furthermore, the simplices of M are partitioned into subtriangulations analogous to the face, edge, and vertex blocks of Chapter 3. Explicit attachment sites are available for (4,2)–handles, so our first step is construction of a (4,2)–handle.

4.3.1 2–handles

The algorithm of this subsection takes as input a pair (T, Γ) where T is a closed solid torus triangulation and Γ is a collection disjoint parallel longitudes in the boundary of T, given as subtriangulations of ∂T. The output is a 4–disk triangulation H satisfying the following:

1. ∂H is a triangulated S^3 with a genus 1 Heegard splitting over ∂T, i.e. T is a subtriangulation of ∂H such that $\partial H \setminus \texttt{int}(T)$ is a solid torus.

2. For each γ_i in Γ, γ_i bounds a triangulated disk in ∂H, i.e. each γ_i is an explicit 0-framing for the (4,2)–handle attachment.

Constructing this disk involves building a solid torus T' that complements T, combining T and T' over their shared boundary to build a triangulated 3–sphere, then coning that 3–sphere into a 4–disk. The resulting disk has a (4,2)–handle structure and we attach it to W over the copy of T contained in its boundary.

We find pairs (T, Γ) inside $M_1 \subset \partial W$, the subdivision of N induced by the subdividing map $f : N \to \mathbb{R}^2$. Let B be a combinatorial face block of M_1. B is a 3–dimensional subtriangulation of M_1 that forms a closed solid torus, and B projects through f over an n–gon for some n. Call the n corners of $f(B)$ by c_i, $i = 1, \ldots, n$, and take $C = \{c_1, \ldots, c_n\}$. Then the $f^{-1}c_i$ are disjoint parallel triangulated longitudes of B. We take $(B, f^{-1}C)$ as our pair (T, Γ) for each combinatorial face block B of M.

For a closed solid torus T, we find a complementary torus T', i.e. $\partial T = \partial T'$ as triangulations. We begin by investigating the boundary of T, setting $T'_0 = \partial T$. Inside T'_0 is the set of disjoint parallel longitudes Γ that are required to bound disks inside T', so for each γ_i we attach a disk D_i with $\partial D_i = \gamma_i$ to T'_0 over γ_i. Call the result of these attachments T'_1. Adjacent longitudes γ_i and γ_j bound an annulus A_{ij} in T'_1, and $D_i \cup A_{ij} \cup D_j$ is a triangulated 2–sphere that we cone into a 3–disk D_{ij}. For each ij, we attach the 3–disk D_{ij} to T'_1 over $D_i \cup A_{ij} \cup D_j$ to form the closed solid torus T'.

By construction $\partial T' = \partial T$, hence the tori are complementary. The longitudinal curves of T, the γ_i, bound triangulated disks in T' thus are meridians of T'. Hence, gluing T and T' over their shared boundary forms a 3–sphere. We then cone that 3–sphere to produce a 4–disk with an explicit (4,2)–handle structure. This is the basic structure of Algorithm 5, which we iterate over the combinatorial face blocks of $M_1 \subset \partial W$. Finally, we attach these handles to W, forming W'.

Let $\mathfrak{B}$ be the collection of combinatorial face blocks of $M_1 \subset \partial W$. Iterating Algorithm 5 over $\mathfrak{B}$ yields a collection of (4,2)–handles $\{H_B^2\}_{B \in \mathfrak{B}}$. The combinatorial face blocks in $\mathfrak{B}$ are disjoint by construction, so we attach our handles in any order. We form the 4–manifold triangulation W' from W as

$$W' = W \cup \{H_B^2\}_{B \in \mathfrak{B}} / \sim,$$

where $\sim$ is defined by $b \sim \iota(b)$, ι the identity map $H_B^2 \supset B \xrightarrow{\iota} B \subset M_1$.

Data: A pair (T, Γ) where T is a closed solid torus triangulation and Γ is a collection of disjoint parallel triangulated longitudes in ∂T

Result: A 4–disk triangulation H_T^2 such that ∂H_T^2 is a triangulated 3–sphere with genus 1 Heegard splitting over ∂T and such that $\gamma_i \in \Gamma$ bounds a triangulated disk in $\partial H_T^2 \setminus \mathtt{int}(T)$ for each i

1 **begin**
2   First, we construct a complementary solid torus T' with $\partial T = \partial T'$
3      $T_0' = \partial T$
4   **foreach** $\gamma_i \in \Gamma$ **do**
5          $D_i^2 = C(\gamma_i)$, the cone of γ_i
6   **end**
7      $T_1' = T_0' \cup \{D_i^2\}/\sim$, where $\sim$ is induced by $\partial D_i^2 = \gamma_i \xrightarrow{\iota} \gamma_i \subset T_0'$
8   **foreach** *adjacent pair of longitudes γ_i, γ_j from Γ* **do**
9          $A_{ij} =$ the annulus in T_1' bounded by γ_i and γ_j
10          $S_{ij}^2 =$ the triangulated 2–sphere in T_1' that is precisely $D_i^2 \cup A_{ij} \cup D_j^2$
11          $D_{ij}^3 = C(S_{ij}^2)$, the cone of S_{ij}^2
12   **end**
13      $T' = T_1' \cup \{D_{ij}^3/\sim\}$, where $\sim$ is induced by $\partial D_{ij}^3 = S_{ij}^2 \xrightarrow{\iota} S_{ij}^2 \subset T_1'$
14      $S_T^3 = T \cup T'/\sim$, where $\sim$ is induced by $\partial T \xrightarrow{\iota} \partial T'$
15      $H_T^2 = C(S_T^3)$, the cone of S_T^3
16 **end**

Algorithm 5: (4,2)–handle construction for a triangulated $S^1 \times D^2$ attachment site

---

The manifold W' is formed by attaching triangulated (4,2)–handles to W over the combinatorial face blocks of M_1. The boundary of W' consists of $M_0 \cup M_1'$, where $M_1' = \partial W' \setminus M_0$ and M_1' is related to M_1 via triangulated (3,2)–handle attachments to M_1 induced by the triangulated (4,2)–handle attachments to W. We decompose M_1' into primed combinatorial edge or vertex block subtriangulations in a manner similar to that found in Chapter 3.

Primed combinatorial edge blocks are the result of attaching triangulated (3,2)–handles over annular boundary components of combinatorial edge blocks. These (3,2)–handles are the triangulated 3-disks D_{ij}^3 formed on Line 11 of Algorithm 5, and their attaching regions are the annuli of combinatorial edge blocks that project through f over edge-face region boundaries.

Let E be a combinatorial edge block. Then E is the product of an orientable surface with an interval, i.e. $E = \Sigma \times [0, 1]$, where Σ is S^2 minus some number of

disjoint open balls. The annuli $\partial\Sigma \times [0,1]$ map through f to edge-face region boundaries, hence these are the attaching sites of (3,2)–handles. Primed combinatorial edge blocks are constructed by performing all such (3,2)–handle attachments, thus each primed combinatorial edge block is a triangulated $S^2 \times [0,1]$.

Differing slightly from Chapter 3, this exhausts the new cells of M_1' introduced by 2–handle attachment. This is due to the different shape of combinatorial vertex regions as compared to the vertex regions of Chapter 3. In Chapter 3 vertex regions were octagonal and shared edge boundaries with face regions. Here, combinatorial vertex regions are quadrilateral and share point boundaries with combinatorial face regions. This point boundary is also shared by a pair of combinatorial edge regions.

Let x be a vertex-face-edge-edge boundary. Then $f^{-1}(x) = \{\gamma^i\}$ is a collection of triangulated circles, and each γ^i is a longitude of a toroidal combinatorial face block in M_1 that projects over the face region whose boundary contains x. Thus, every γ^i has been filled by a 2–disc constructed on Line 5 of Algorithm 5. Each of these new disks has been assigned to two primed combinatorial edge blocks, but we will also assign them to the primed vertex block that contains γ^i.

This means that each primed combinatorial vertex block is now equivalent to a triangulated (3,2)–handlebody. Let V be a combinatorial vertex block and V' be V primed. Considering each new disc in V' to be a flattened (3,2)–handle, we conclude that V' is a (3,2)–handlebody using the argument found in Theorem 3.4.1. Restating a sketch of that argument here, the attaching spheres of (3,2)–handles transversely intersect the belt spheres of the (3,1)–handles at most once, each belt sphere intersects at least one attaching sphere and vice versa, and the boundary of V' is a disjoint collection of 2–spheres, thus V' is a (3,2)–handlebody.

4.3.2   3–handles

We now construct (4,3)–handles to attach over our primed combinatorial edge blocks. Let E' be such a block. Then $\partial E'$ is a disjoint pair of triangulated 2–spheres. We form a 4–disk containing E' in its boundary by a double coning method on E': we first cone the spherical boundary components of E' to form a pair of triangulated 3–disks, glue these 3–disks to E' to form a 3–sphere, then cone the 3–sphere to obtain a 4–disk. This idea is identical to that found in Section 3.4.2 and is formalized in Algorithm 6. Finally, we attach (4,3)–handles built using Algorithm 6 to W' over primed combinatorial edge blocks.

Let $\mathfrak{E}'$ be the collection of primed combinatorial edge blocks of $M_1' \subset \partial W'$. Iterating Algorithm 6 over $\mathfrak{E}'$ yields a collection of (4,3)–handles $\{H_{E'}^3\}_{E' \in \mathfrak{E}'}$. The primed combinatorial edge blocks in $\mathfrak{E}'$ intersect only in discs that are also shared by primed combinatorial vertex blocks and these disks are invariant under the (4,3)–handle attachment so we attach our handles in any order. We form the 4–manifold triangulation W'' from W' as

$$W'' = W' \cup \{H_{E'}^3\}_{E' \in \mathfrak{E}'} / \sim,$$

where $\sim$ is defined by $e \sim \iota(e)$, ι the identity map $H_{E'}^3 \supset E' \xrightarrow{\iota} E' \subset M_1'$.

Data: E', a triangulated $S^2 \times [0,1]$
Result: A 4–disk triangulation $H_{E'}^3$ such that $\partial H_{E'}^3$ is a triangulated
    3–sphere containing E' as a subtriangulation
1 **begin**
2   First, we attach 3–disks to E' over its two 2-sphere boundary components
3   **foreach** *boundary sphere* $S_i^2 \in \partial E'$ **do**
4      $C(S_i^2) = $ the cone of S_i^2
5   Attach $C(S_i^2)$ to $\partial E'$ over $S_i^2 \in \partial E'$
6   **end**
7   The result of the above attachments is the 3–sphere $S_{E'}^3$
8   Then $H_{E'}^3 = C(S_{E'}^3)$
9 **end**

Algorithm 6: (4,3)–handle construction for a triangulated $S^2 \times [0,1]$ attachment site

---

The manifold W'' is formed by attaching triangulated (4,3)–handles to W' over the primed combinatorial edge blocks of M_1'. The boundary of W'' consists of $M_0 \cup M_1''$, where $M_1'' = \partial W'' \setminus M_0$ and M_1'' is related to M_1' via triangulated (3,3)–handle attachments to M_1' induced by the triangulated (4,3)–handle attachments to W'. These (3,3)–handle attachments turn primed combinatorial vertex blocks into double primed combinatorial vertex blocks. A primed combinatorial vertex block is a (3,2)–handlebody, so a double primed combinatorial vertex block is a (3,2)–handlebody with each S^2 boundary component filled in with a (3,3)–handle, thus each double primed combinatorial vertex block is a triangulated S^3.

4.3.3 4–handles

We now construct (4,4)–handles to attach over our double primed combinatorial vertex blocks. Let V'' be such a block. Then V'' is a triangulated S^3, so a (4,4)–handle structure that can be attached over V'' is constructed by coning V''. This is made explicit in Algorithm 7, which serves double duty as a general algorithm for coning spheres into discs. These handles are attached to W'' to form a triangulated 4–manifold whose only boundary component is M_0.

Let $\mathfrak{V}''$ be the collection of double primed combinatorial vertex blocks of $M_1'' \subset \partial W''$. Coning each element of $\mathfrak{V}''$ yields a collection of (4,4)–handles $\{H_{V''}^4\}_{V'' \in \mathfrak{V}''}$. The double primed combinatorial vertex blocks in $\mathfrak{V}''$ are disjoint, so we attach our handles in any order. We form the 4–manifold triangulation W''' from W'' as

$$W''' = W'' \cup \{H_{V''}^4\}_{V'' \in \mathfrak{V}''} / \sim,$$

where $\sim$ is defined by $v \sim \iota(v)$, ι the identity map $H_{V''}^4 \supset V'' \overset{\iota}{\to} V'' \subset M_1''$.

Data: V'', a triangulated S^3
Result: A 4–disk triangulation $H_{V''}^4$ such that $\partial H_{V''}^4 = V''$
1 **begin**
2 $\quad H_{V''}^4 = V''$
3 $\quad$ Add a 0–cell x to $H_{V''}^4$
4 $\quad$ **for** $i = 0, \ldots, 3$ **do**
5 $\quad\quad$ **foreach** i–cell y of $V'' \subset H_{V''}^4$ **do**
6 $\quad\quad\quad Z(y) = \{z \in H_{V''}^4 \mid z \notin V''$ and $\partial z \cap \partial y \neq \emptyset\}$
7 $\quad\quad\quad$ Attach an $(i+1)$–cell to $H_{V''}^4$ over $y \cup Z(y) \cup x$
8 $\quad\quad$ **end**
9 $\quad$ **end**
10 **end**

Algorithm 7: (4,4)–handle construction for a triangulated S^3 attachment site; equivalently, coning a 3–sphere

---

The triangulated 4–manifold W''' has only one boundary component: M_0. By construction, M_0 is equivalent to the original input 3–manifold triangulation N by subdivision of N, hence W''' is a triangulated 4–manifold with boundary N, as desired. Each algorithm in the construction is now chained together in Algorithm 8.

Data: N, a 3–manifold triangulation

Result: A 4–manifold triangulation whose boundary is equivalent to N through subdivision

1 begin

2   Obtain a subdiving map f for N from Algorithm 1

3   Construct N', a 3–dimensional cell complex equivalent to N from Algorithm 2 applied to (N, f)

4 N' is a polyhedral gluing, so we obtain an equivalent triangulation M by applying Algorithm 3 to N'

5   Form the 4–thickening $W = M \times I$ by applying Algorithm 4 to M

6 $\mathfrak{B}$ = the collection of combinatorial face blocks of $M_1 \subset \partial W$

7   **foreach** $B \in \mathfrak{B}$ **do**

8 H_B^2 = the (4,2)–handle produced by Algorithm 5 applied to B

9   **end**

10 W' = the 4–manifold triangulation obtained by attaching H_B^2 to W over B for each $B \in \mathfrak{B}$

11 $M_1' = \partial W' \setminus M_0$

12   Apportion the cells of $\{H_B^2\}_{B \in \mathfrak{B}}$ to the combinatorial edge and vertex blocks of W' to form primed combinatorial edge and vertex blocks

13 $\mathfrak{E}'$ = the collection of primed combinatorial edge blocks of $M_1' \subset \partial W'$

14   **foreach** $E' \in \mathfrak{E}'$ **do**

15 $H_{E'}^3$ = the (4,3)–handle produced by Algorithm 6 applied to E'

16   **end**

17 W'' = the 4–manifold triangulation obtained by attaching $H_{E'}^3$ to W' over E' for each $E' \in \mathfrak{E}'$

18 $M_1'' = \partial W'' \setminus M_0$

19   Apportion the cells of $\{H_{E'}^3\}_{E' \in \mathfrak{E}'}$ to the primed combinatorial vertex blocks of W'' to form double primed combinatorial vertex blocks

20 $\mathfrak{V}''$ = the collection of double primed combinatorial vertex blocks of $M_1'' \subset \partial W''$

21   **foreach** $V'' \in \mathfrak{V}''$ **do**

22 $H_{V''}^4$ = the (4,4)–handle produced by Algorithm 7 applied to V''

23   **end**

24 W''' = the 4–manifold triangulation obtained by attaching $H_{V''}^4$ to W'' over V'' for each $V'' \in \mathfrak{V}''$

25 $\partial W''' = M_0$ and $M_0 \equiv N$ through subdivision

26   **return** W'''

27 end

Algorithm 8: Full construction of a triangulated 4–manifold with prescribed 3–manifold boundary

Chapter 5

Discussion

The main chapters of this thesis serve different roles in the greater mathematical ecosystem. It is evident from the discussion in Section 2.2 of [4] that the ideas behind the constructive proof in Chapter 3 are not novel, but the details had yet to be published. Chapter 3 fills a hole in the current literature, whereas the contents of Chapter 4 are entirely new, serving as a solid foundation for future research in computational topology.

The immediate next step from creation of the algorithm is an implementation for a topology software project such as Regina [1]. Such an implementation furthers progress toward algorithmic computation of the Rokhlin invariant for 3–manifolds and serves as another tool in generating 4–manifold censuses. In its current form, the construction algorithm guarantees no topological features of the constructed 4–manifold save that its boundary is the given input 3–manifold. Lucrative avenues of exploration would therefore include an investigation into invariants (e.g. the fundamental group) or constructs (e.g. spin structures) on the constructed manifold.

This work was initially an attempt to adapt the Turaev Reconstruction Theorem as an algorithm on 3–manifolds triangulations. The theorem was introduced by Turaev [14] and is also covered by Costantino [3]. The algorithm would build on the process outlined in Chapter 4 of Costantino and Thurston [4], where a quadratic bound is achieved for the number of simplices needed to triangulate a 4–manifold constructed using the reconstruction theorem.

Such an adaptation necessarily passes through the shadow realm. The shadows explored in [14] are 2–complexes with strict structural restrictions imposed upon them. In the reconstruction theorem, a shadow serves as a set of instructions for a handle decomposition of the desired 4–manifold. Each 0–cell prescribes a (4,0)–handle, each

1–cell a (4,1)–handle, and each 2–cell a (4,2)–handle. The resulting 4–manifold W has boundary exactly the original 3–manifold M. Two major obstructions eventually caused this adaptation attempt to be scrapped:

1. Precisely defining (4,2)–handle attachment sites in this process is difficult.

2. The fact that $\partial W = M$ at the end of this process is not obvious and requires a deep examination of shadows (briefly, $\partial W = M$ because M and W have the same shadow).

Instead, the results of this work were obtained by turning the reconstruction theorem on its head: we begin by making the precise definition of (4,2)–handle attachment sites as simple as possible. Once (4,2)–handles have been attached, attachment of (4,3)– and (4,4)–handles is straightforward. This method is dual to the Turaev Reconstruction Theorem in its approach and handle indexing $((n, \lambda)$– and $(n, n - \lambda)$–handles are identical, just attached over complementary portions of the handle's boundary), but the goals are different. Turaev's work is focused on studying the topology of the shadows themselves, where our ultimate goal is algorithmic construction of 4–manifolds with prescribed boundary.

Beyond its raw results, this research is a demonstration of adapting an existence proof into a constructive proof. More adaptations of existence proofs should not be surprising as the bounds of scientific computability are pushed.

Bibliography

[1] Benjamin Burton, Ryan Budney, William Pettersson, et al. Regina: Software for low-dimensional topology. `http://regina.sourceforge.net/`, 1999–2019.

[2] Benjamin A Burton. Simplification paths in the pachner graphs of closed orientable 3-manifold triangulations. *arXiv preprint arXiv:1110.6080*, 2011.

[3] Francesco Costantino. A short introduction to shadows of 4–manifolds. `https://arxiv.org/abs/math/0405582/`, 2005.

[4] Francesco Costantino and Dylan Thurston. 3-manifolds efficiently bound 4-manifolds. *Journal of Topology*, (3) 1, 2008.

[5] Marc Culler, Nathan M. Dunfield, and Jeffrey R. Weeks. Snappy, a computer program for studying the geometry and topology of 3-manifolds, 2017.

[6] Robert Gompf and Andràs Stipsicz. *4–Manifolds and Kirby Calculus*. American Mathematical Society, 1999.

[7] John M. Lee. *Introduction to Smooth Manifolds*. Springer, 2000.

[8] Harold Levine. Elimination of cusps. *Topology*, 3(2):263–296, 1965.

[9] Bjorn Poonen and Michael Rubinstein. The number of intersection points made by the diagonals of a regular polygon. *SIAM Journal on Discrete Mathematics*, (1) 11:135–156, 1998.

[10] Osamu Saeki. Constructing generic smooth maps of a manifold into a surface with prescribed singular loci. *Annales de l'Institut Fourier*, 45(4):1135–1162, 1995.

[11] Osamu Saeki. *Topology of Singular Fibers of Differentiable Maps*. Lecture Notes in Mathematics 1854. Springer, 2004.

[12] Saul Schleimer. Waldhausen's theorem. *Geometry & Topology Monographs*, 12:299–317, 2007.

[13] William P Thurston. *The geometry and topology of three-manifolds.* Princeton University Princeton, NJ, 1979.

[14] Vladimir Turaev. Topology of shadows, 1991. Preprint.

[15] Shmuel Weinberger. *The topological classification of stratified spaces.* Chicago, 1994.